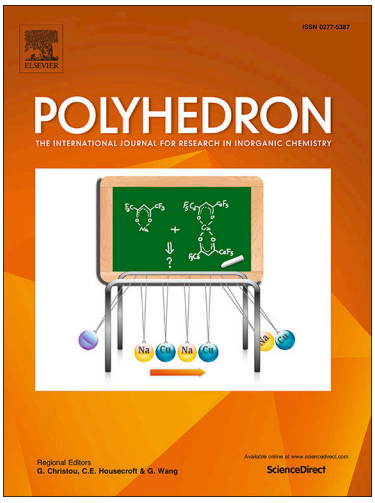

Tin(IV) compounds of tridentate thiosemicarbazone Schiff bases: synthesis, characterization, *in-silico* analysis and *in vitro* cytotoxicity

Enis Nadia Md Yusof, Alister J. Page, Jennette A. Sakoff, Michela I. Simone, Abhi Veerakumarasivam, Edward R.T. Tiekink, Thahira B.S.A. Ravoof

PII: S0277-5387(20)30386-7
DOI: https://doi.org/10.1016/j.poly.2020.114729
Reference: POLY 114729

To appear in: *Polyhedron*

Received Date: 2 July 2020
Revised Date: 28 July 2020
Accepted Date: 30 July 2020

Please cite this article as: E.N.M. Yusof, A.J. Page, J.A. Sakoff, M.I. Simone, A. Veerakumarasivam, E.R.T. Tiekink, T.B.S. Ravoof, Tin(IV) compounds of tridentate thiosemicarbazone Schiff bases: synthesis, characterization, *in-silico* analysis and *in vitro* cytotoxicity, *Polyhedron* (2020), doi: https://doi.org/10.1016/j.poly.2020.114729

Tin(IV) compounds of tridentate thiosemicarbazone Schiff bases: synthesis, characterization, *in-silico* analysis and *in vitro* cytotoxicity

Enis Nadia Md Yusof [1,2,3], Alister J. Page [2,*], Jennette A. Sakoff [4], Michela I. Simone [2,5], Abhi Veerakumarasivam [6,7], Edward R. T. Tiekink [8] and Thahira B. S. A. Ravoof [1,9,*]

[1] Department of Chemistry, Faculty of Science, Universiti Putra Malaysia, 43400 UPM Serdang, Selangor, Malaysia;
[2] Discipline of Chemistry, School of Environmental and Life Sciences, University of Newcastle, University Drive, Callaghan, NSW 2308, Australia;
[3] Chemistry Section, School of Distance Education, Universiti Sains Malaysia, 11800, Minden, Penang, Malaysia
[4] Experimental Therapeutics Group, Department of Medical Oncology, Calvary Mater Newcastle Hospital, Edith Street, Waratah NSW 2298, Australia;
[5] Priority Research Centre for Drug Development, University of Newcastle, University Drive, Callaghan, NSW 2308, Australia
[6] Department of Biological Sciences, School of Science and Technology, Sunway University, No. 5 Jalan Universiti, 47500 Bandar Sunway, Selangor Darul Ehsan, Malaysia;
[7] Medical Genetics Laboratory, Faculty of Medicine and Health Sciences, Universiti Putra Malaysia, 43400 UPM Serdang, Selangor Darul Ehsan, Malaysia
[8] Research Centre for Crystalline Materials, School of Science and Technology, Sunway University, No. 5 Jalan Universiti, 47500 Bandar Sunway, Selangor Darul Ehsan, Malaysia;
[9] Foundry of Reticular Materials for Sustainability (FORMS), Materials Synthesis and Characterization Laboratory, Institute of Advanced Technology, Universiti Putra Malaysia, 43400 Serdang, Selangor Darul Ehsan, Malaysia;

***** Correspondence: thahira@upm.edu.my (T.B.S.A.R.), alister.page@newcastle.edu.au (A.J.P.)

Abstract

Twelve tin(IV) compounds (**5-16**) derived from four tridentate thiosemicarbazone Schiff bases of 4-methyl-3-thiosemicarbazide with 2-hydroxy-3-methoxybenzaldehyde (**1, 2**) and 4-phenyl-3-thiosemicarbazide with 2,3-dihydroxybenzaldehyde (**3, 4**) of the general formulae $[R_2Sn(L^n)]$ and $[Sn(L^n)_2]$ (where R = Ph or Me; L^n = **1**, **2**, **3** and **4**) were synthesized and characterized by elemental analysis, IR, UV-vis, mass spectrometry and multinuclear NMR (^1H, ^{13}C and ^{119}Sn) spectroscopy. X-ray crystallographic data was obtained for **11′**, a 2:1 co-crystal between $Ph_2Sn(L^2)$ (**11**) and 3-methoxysalicylaldehyde azine, and $Me_2Sn(L^2)$ (**12**)

where L^2H_2 is 2-(2-hydroxy-3-methoxybenzylidene)-N-phenylhydrazinecarbothioamide. The analysis revealed distinct coordination geometries for **11** and **12** approaching trigonal-bipyramidal. In the crystal of **11′**, supramolecular dimers arising from amine-N–H···S(thiolate) hydrogen bonding and $\{\cdots HNCS\}_2$ synthons are evident; π(chelate ring)···π(oxidobenzylidene) stacking is also apparent. In the crystal of **12**, supramolecular, helical chains are generated by a combination of amine-N–H···O(phenoxide) hydrogen bonding and Sn···S secondary bonding. The cytotoxic activity of the compounds against a panel of ten cancer cell lines, [HT29 (colon), U87 and SJ-G2 (glioblastoma), MCF-7 (breast), A2780 (ovarian), H460 (lung), A431 (skin), DU145 (prostate), BE2-C (neuroblastoma) and MIA (pancreas), and one normal cell line, MCF-10A (normal breast)] were investigated. The thiosemicarbazone Schiff bases **1** and **4** as well as the diphenyltin(IV) compounds showed a strong ability to inhibit the growth of cancer cells, with particular selectivity against HT29, MCF-7, A2780, A431, BE2-C, SJ-G2 and MIA cell lines. The structure-activity relationship of all these compounds were studied by evaluating the effect of alkyl and aryl groups attached on the thiosemicarbazone backbone, the methoxy/hydroxyl groups present at the *meta*-position of the phenyl ring and alkyl or aryl groups bound to the tin center.

1. Introduction

Schiff bases that contain nitrogen, sulfur and oxygen as donor atoms, such as thiosemicarbazones, semicarbazones and dithiocarbazates, and their metal complexes have been of interest since 1946 [1] owing to their remarkable biological and pharmacological properties, especially antitumor, antibacterial, antiviral, anti-tuberculosis, antifungal and antimalarial activities [2], which are altered when small changes to the structures (e.g., changing of a functional group) are applied. Thiosemicarbazones are considered as privileged ligands due to their potential donor atoms, π-delocalization and configurational flexibility, which can produce various metal-ligand linkages [3]. Compounds having thiol groups have also been proven to inhibit the ribonucleotide reductase (RR) enzyme, used in DNA synthesis. Hence, by inhibiting or blocking the function of the RR enzyme, DNA replication and synthesis of tumor cells can be controlled or prevented [4]. In many cases, complexation with metal ions increases the bioactivity of the compounds, suggesting that coordination of such ligands enhances their cytotoxicity.

Although much research has been devoted to the synthesis, characterization and biological properties of ligands coordinated to transition metal ions, tin-based compounds have received considerably less attention because of ecotoxicology effects at the biochemical, cellular and organism levels [5]. In recent years, tin-based compounds have been of great interest because of their ability to form stable bonds with hetero donor atoms, for instance nitrogen, sulfur and oxygen atoms [6–15]. Tin(IV) compounds are now well-known for their applications as cytotoxic, biocidal, antibacterial and antifungal agents [6,16–19]. Many studies have reported the antimicrobial activities of tin(IV) compounds derived from thiosemicarbazone Schiff bases. In particular, compounds containing the 3-methoxysalicylaldehyde thiosemicarbazone Schiff base were tested for their *in vitro* cytotoxicity against human acute lymphoblastic leukemia (Jurkat cells) [20]. The data indicated increasing potency in the order dimethyltin(IV) < diphenyltin(IV) < dibutyltin(IV) compounds, with IC_{50} values of 260, 130 and 50 μM, respectively. This suggested that the cytotoxicity of dialkytin(IV) compounds increased with the increase in the length of the organic chain. The cytotoxicity of diphenyl- and dimethyltin(IV) compounds of pyruvic acid thiosemicarbazone have also been investigated against human breast adenocarcinoma (MCF-7), bladder carcinoma (T24), non-small cell lung carcinoma (A-549) and mouse fibroblast (L-929) cell lines, with IC_{50} values in the range 0.43 to 19.73 μM. The diphenyltin(IV) compound was most potent against T-24 cells with an IC_{50} value of 0.43 μM, where it exhibited 96-fold better activity than cisplatin [21].

Recently, tin(IV) compounds derived from the tridentate 2-hydroxy-5-methoxybenzaldehyde-N(4)-methylthiosemicarbazone exhibited higher anticancer activity against the human colorectal (HTC-116) cell line as compared to the reference drug 5-fluorouracil [8]. The significant biological activity of the tin(IV) compounds were influenced by the types of organo group attached to the tin center, diffusion, lipophilicity and steric effects [8,22–24].

As a continuation of our research on tridentate ONS Schiff bases and their tin(IV) compounds [25,26], we report herein the preparation, spectroscopic characterization and bioactivity of tin(IV) compounds (**5**-**16**) containing 2-hydroxy-3-methoxybenzyl- and 2,3-dihydroxybenzyl-derived thiosemicarbazone Schiff bases (**1**-**4**). The diphenyl- (**5**, **8**, **11**, and **14**) and dimethyltin(IV) (**6**, **9**, **12**, and **15**) compounds exhibited a penta-coordinated geometry, whereas tin(IV) compounds were coordinated to two molecules of thiosemicarbazone Schiff

bases (**7**, **10**, **13**, and **16**) suggesting a hexa-coordinated geometry, according to ^{119}Sn NMR analysis.

The experimental data (FTIR, electronic and single crystal X-ray diffraction analysis) of the synthesized compounds were in excellent agreement with the computed data, as evidenced by density functional theory (DFT) calculations using the B3LYP/LanL2DZ/6-311G(*d*,*p*) level of theory. The cytotoxicity of all the compounds against a panel of ten cancer cell lines and one normal cell line was investigated. The results indicated that small differences in the structures of the compounds (Figure 1) had significant effects on their activity. These studies provide fundamental data for future drug design development in cancer treatment.

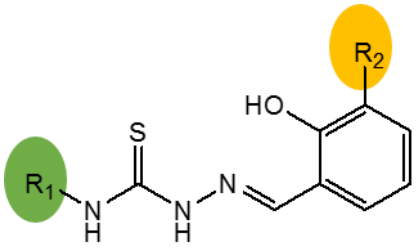

$R_1 = CH_3$, $R_2 = OCH_3$ (**1**)
$R_1 = C_6H_5$, $R_2 = OCH_3$ (**2**)
$R_1 = CH_3$, $R_2 = OH$ (**3**)
$R_1 = C_6H_5$, $R_2 = OH$ (**4**)

Figure 1. The structure of the thiosemicarbazone Schiff bases **1**-**4**.

2. Experimental

2.1. Physical measurements

Melting points were determined using an Electrothermal digital melting point apparatus. IR spectra were recorded using the Perkin Elmer Spectrum 100 with Universal ATR Polarization in the range 4000–280 cm^{-1}. C, H and N elemental analyses were carried out using a LECO CHNS-932 instrument. Molar conductivities of 10^{-3} M solutions of the organotin(IV) compounds in DMSO were measured at 27 °C using a Jenway 4310 conductivity meter fitted with a dip-type cell with a platinized electrode. Electronic spectra were recorded on a Shimadzu UV-1650 PC recording spectrophotometer (1000–200 nm). ^{1}H and ^{13}C NMR spectra were recorded using an NMR JNM ECA400 spectrometer. ^{119}Sn NMR were measured using a Bruker BioSpin Avance III (600MHz) spectrometer. The mass spectra were recorded using a Shimadzu GC-MS QP2010Plus mass spectrometer.

2.2. Materials

All solvents and reagents were of analytical reagent grade and used without further purification.

Chemicals: 4-methyl-3-thiosemicarbazide, 4-phenyl-3-thiosemicarbazide, potassium hydroxide, 2-hydroxy-3-methoxybenzaldehyde, 2,3-dihydroxybenzaldehyde, dichlorodiphenyltin(IV), dichlorodimethyltin(IV), tin(II) chloride. Solvents: absolute ethanol, 99.8%, ethanol, 95%, methanol, dimethylsulfoxide.

2.3. Syntheses

*2.3.1. Syntheses of 2-(2-hydroxy-3-methoxybenzylidene)-N-methylhydrazinecarbothioamide (**1**) and 2-(2-hydroxy-3-methoxybenzylidene)-N-phenylhydrazinecarbothioamide (**2**)*

Compounds **1** and **2** were prepared according to the procedure described in the literature [27,28] with some modifications.

4-Methylthiosemicarbazide (1.05 g, 10 mmol)/4-phenylthiosemicarbazide (1.67 g, 10 mmol) was dissolved in methanol (40 cm^3) with stirring and heating (40 °C) over a period of 30 minutes. 3-Methoxysalicylaldehyde (1.52 g, 10 mmol) in 10 cm^3 of methanol was added to the thiosemicarbazide solution and stirred at room temperature for 4 h. Upon cooling, a crystalline product began to form which was filtered, washed with cold methanol and dried in a desiccator over anhydrous silica gel.

*2-(2-Hydroxy-3-methoxybenzylidene)-N-methylhydrazinecarbothioamide (**1**)*

Colorless crystalline solid. Yield: 92 %. Melting point: 242-243 °C. Analysis calculated for $C_{10}H_{13}N_3O_2S$: C, 50.19; H, 5.48; N, 17.56. Found: C, 49.93; H, 5.38; N, 17.22 %. FT-IR (ATR, cm^{-1}): 3337 *ν*(OH), 3304 *ν*(NH), 1610 *ν*(C=N), 1109 *ν*(N-N), 1037 *ν*(C=S). ^{1}H NMR (DMSO-d_6) δ (ppm.): 2.99 (d, 3H, CH_3), 3.79 (s, 3H, O-CH_3), 6.93-7.54 (m, 3H, Ar-H), 8.37 (s, 1H, CH), 8.39 (q, 1H, C(=S)-NH), 9.18 (s, 1H, OH), 11.42 (s, 1H, NH-N). ^{13}C NMR (DMSO-d_6) δ (ppm.): 30.8 (N-CH_3), 56.4 (O-CH_3), 113.1, 118.2, 119.2, 121.2, 139.6, 146.7 (Ar-C), 148.4 (C=N), 177.6 (C=S).

*2-(2-Hydroxy-3-methoxybenzylidene)-N-phenylhydrazinecarbothioamide (**2**)*

White crystalline solid. Yield: 90 %. Melting point: 209-210 °C. Analysis calculated for $C_{15}H_{15}N_3O_2S$: C, 59.78; H, 5.02; N, 13.94. Found: C, 59.99; H, 5.15; N, 13.80 %. FT-IR (ATR, cm^{-1}): 3300 *ν*(NH), 1609 *ν*(C=N), 1103 *ν*(N-N), 908 *ν*(C=S). ^{1}H NMR (DMSO-d_6) δ

(ppm.): 3.80 (s, 3H, O-CH_3), 6.77-7.69 (m, 8H, Ar-H), 9.26 (s, 1H, CH), 10.02 (s, 1H, OH), 11.78 (s, 1H, NH-N). ^{13}C NMR (DMSO-d_6) δ (ppm.): 56.3 (O-CH_3), 113.4, 118.8, 119.5, 121.2, 125.4, 126.4, 128.6, 139.7, 140.4, 146.6 (aromatic-C), 148.6 (C=N), 176.1 (C=S).

*2.3.2. Syntheses of 2-(2,3-dihydroxybenzylidene)-N-methylhydrazinecarbothioamide (**3**) and 2-(2,3-dihydroxybenzylidene)-N-phenylhydrazinecarbothioamide (**4**)*

Compounds **3** and **4** were prepared according to the procedure described in the literature [29,30]. A 25 cm^3 ethanolic solution of 2,3-dihydroxybenzaldehyde (1.38 g, 10 mmol) was added to an equimolar ethanolic solution (10 cm^3) of 4-methyl-3-thiosemicarbazide (1.05 g, 10 mmol)/4-phenyl-3-thiosemicarbazide (1.67 g, 10 mmol). The mixture was stirred for 3 hours at room temperature and the title compound was filtered. Each of the title compounds was then recrystallized from methanol to remove all the impurities and kept in desiccator over anhydrous silica gel.

*2-(2,3-Dihydroxybenzylidene)-N-methylhydrazinecarbothioamide (**3**)*

Pale yellow solid. Yield: 83 %. Melting point: 231-232 °C. Analysis calculated for $C_9H_{11}N_3O_2S$: C, 47.99; H, 4.92; N, 18.65. Found: C, 46.88; H, 4.85; N, 18.38 %. FT-IR (ATR, cm^{-1}): 3418 *ν*(OH), 3140 *ν*(NH), 1601 *ν*(C=N), 1112 *ν*(N-N), 1035 *ν*(C=S). ^{1}H NMR (DMSO-d_6) δ (ppm.): 3.00 (d, 3H, CH_3), 6.67-7.38 (m, 3H, Ar-H), 9.02 (s, 1H, CH), 8.37, 8.38 (2 x s, 2H, OH), 9.49 (s, 1H, C(=S)-NH), 11.40 (s, 1H, NH-N). ^{13}C NMR (DMSO-d_6) δ (ppm.): 31.3 (N-CH_3), 116.7, 117.4, 119.4, 121.5, 140.1, 145.6 (Ar-C), 146.0 (C=N), 178.0 (C=S).

*2-(2,3-Dihydroxybenzylidene)-N-phenylhydrazinecarbothioamide (**4**)*

Pale yellow solid. Yield: 70 %. Melting point: 215-216 °C. Analysis calculated for $C_{14}H_{13}N_3O_2S$: C, 58.52; H, 4.56; N, 14.62. Found: C, 57.61; H, 4.69; N, 14.67 %. FT-IR (ATR, cm^{-1}): 3443 *ν*(OH), 3129 *ν*(NH), 1597 *ν*(C=N), 1047 *ν*(N-N), 1029 *ν*(C=S). ^{1}H NMR (DMSO-d_6) δ (ppm.): 6.67-7.57 (m, 8H, Ar-H), 8.49 (s, 1H, CH), 8.96, 9.52 (2 x s, 2H, OH), 10.01 (s, 1H, C(=S)-NH), 11.75 (s, 1H, NH-N). ^{13}C NMR (DMSO-d_6) δ (ppm.): 117.1, 117.9, 119.5, 121.3, 125.6, 126.0, 128.5, 139.6, 141.3, 145.9 (Ar-C), 146.0 (C=N), 176.0 (C=S).

*2.3.3. General procedure for the synthesis of tin(IV) compounds derived from **1** and **3***

To a solution of **1** (0.24 g, 1 mmol)/ **3** (0.23 g, 1 mmol) in 100 cm^3 of methanol, KOH (0.11 g, 2 mmol) was added and the mixture was stirred and heated for 30 minutes in methanol. Then, 1 mmol of the tin precursor (Ph_2SnCl_2 (0.34 g)/ Me_2SnCl_2 (0.22 g)/ $SnCl_2$ (0.19 g)) was added to the mixture and refluxed for 2 hours under nitrogen. The mixture was filtered while hot and then the filtrate was placed in a freezer until a bright yellow solid formed. The solid residue obtained was recrystallized from methanol.

*Diphenyltin(IV) compound of 2-(2-hydroxy-3-methoxybenzylidene)-N-methylhydrazine carbothioamide (**5**)*

Bright yellow solid. Yield: 74 %. Melting point: 138-139 °C. Analysis calculated for $C_{22}H_{21}N_3O_2SSn$: C, 51.79; H, 4.15; N, 8.24. Found: C, 51.03; H, 4.23; N, 8.16 %. FT-IR (ATR, cm^{-1}): 3299 *ν*(N-H), 1596 *ν*(C=N), 1066 *ν*(N-N), 973 *ν*(C=S). ^{1}H NMR ($CDCl_3$) δ (ppm.): 3.01 (d, 3H, N-CH_3), 3.96 (s, 3H, O-CH_3), 7.96 (s, 1H, CH), 7.36-8.12 (m, 13H, Ar-H), 8.59 (s, 1H, NH). ^{13}C NMR ($CDCl_3$) δ (ppm.): 29.8 (NH-CH_3), 56.5 (O-CH_3), 115.7, 116.7, 117.2, 125.1, 128.6, 129.9, 135.9, 142.5, 151.6 (Ar-C), 157.1 (C=N), 160.3 (S-C-S). ^{119}Sn NMR ($CDCl_3$) δ (ppm.): -236.

*Dimethyltin(IV) compound of 2-(2-hydroxy-3-methoxybenzylidene)-N-methylhydrazine carbothioamide (**6**)*

Bright yellow solid. Yield: 42 %. Melting point: 164-168 °C. Analysis calculated for $C_{12}H_{17}N_3O_2SSn$: C, 37.33; H, 4.44; N, 10.88. Found: C, 39.00; H, 4.76; N, 11.00 %. FT-IR (ATR, cm^{-1}): 3222 *ν*(N-H), 1590 *ν*(C=N), 1066 *ν*(N-N), 973 *ν*(C=S). ^{1}H NMR ($CDCl_3$) δ (ppm.): 0.91 (s, 6H, Sn-CH_3), 2.97 (d, 3H, N-CH_3), 3.94 (s, 3H, O-CH_3), 7.26 (s, 1H, CH), 6.66-6.87 (m, 3H, Ar-H), 8.55 (s, 1H, NH). ^{13}C NMR ($CDCl_3$) δ (ppm.): 8.7 (Sn-CH_3), 31.3 (NH-CH_3), 56.4 (O-CH_3), 115.7, 115.8, 117.8, 118.5, 125.8, 151.3 (Ar-C), 156.5 (C=N), 178.0 (S-C-S). ^{119}Sn NMR (DMSO-d_6) δ (ppm.): -154.

*Tin(IV) compound of 2-(2-hydroxy-3-methoxybenzylidene)-N-methylhydrazine carbothioamide (**7**)*

Compound **7** was prepared following the same procedure as described for **5**, using **1** (0.48 g, 2 mmol). Bright yellow solid. Yield: 31 %. Melting point: 118-119 °C. Analysis calculated for $C_{20}H_{22}N_6O_4S_2Sn$: C, 40.49; H, 3.74; N, 14.17. Found: C, 40.50; H, 3.33; N, 14.17 %. FT-

IR (ATR, cm^{-1}): 3308 *v*(N-H), 1590 *v*(C=N), 1066 *v*(N-N), 973 *v*(C=S). ^{1}H NMR (DMSO-d_6) δ (ppm.): 2.36 (d, 6H, N-CH_3), 3.82 (s, 6H, O-CH_3), 7.60 (s, 2H, CH), 6.67-7.31 (m, 6H, Ar-H), 8.88 (s, 2H, NH). ^{13}C NMR (DMSO-d_6) δ (ppm.): 19.3 (NH-CH_3), 56.7 (O-CH_3), 105.4, 116.7, 117.4, 126.5, 128.6, 129.0, 130.7, 130.8, 134.9, 149.7, 151.8, 158.3 (Ar-C), 163.7 (C=N), 170.6 (S-C-S). ^{119}Sn NMR (DMSO-d_6) δ (ppm.): -354.

*Diphenyltin(IV) compound of 2-(2,3-dihydroxybenzylidene)-N-methylhydrazine carbothioamide (**8**)*

Yellow solid. Yield: 49 %. Melting point: 186-192 °C. Analysis calculated for $C_{21}H_{19}N_3O_2SSn$: C, 50.83; H, 3.86; N, 8.47. Found: C, 48.06; H, 4.27; N, 8.02 %. FT-IR (ATR, cm^{-1}): 1593 *v*(C=N), 1006 *v*(N-N), 953 *v*(C=S). ^{1}H NMR (DMSO-d_6) δ (ppm.): 3.00 (s, 3H, NH-CH_3), 8.57 (s, 1H, CH), 6.37-8.20 (m, 13H, Ar-H), 11.27 (s, 1H, NH). ^{13}C NMR (DMSO-d_6) δ (ppm.): 30.9 (NH-CH_3), 112.8, 113.7, 115.7, 118.4, 128.3, 129.2, 136.0, 136.1, 141.1, 145.4, 153.3 (aromatic-C), 154.3 (C=N), 177.0 (S-C-S). ^{119}Sn NMR (DMSO-d_6) δ (ppm.): -227.

*Dimethyltin(IV) compound of 2-(2,3-dihydroxybenzylidene)-N-methylhydrazine carbothioamide (**9**)*

Yellow solid. Yield: 32 %. Melting point: 223-225 °C. Analysis calculated for $C_{11}H_{15}N_3O_2SSn$: C, 35.51; H, 4.06; N, 11.29. Found: C, 35.87; H, 3.86; N, 11.35 %. FT-IR (ATR, cm^{-1}): 1596 *v*(C=N), 1006 *v*(N-N), 951 *v*(C=S). ^{1}H NMR (DMSO-d_6) δ (ppm.): 0.62 (s, 6H, Sn-CH_3), 3.00 (d, 3H, N-CH_3), 6.32-7.10 (m, 3H, Ar-H), 8.38 (s, 1H, CH), 11.30 (s, 1H, NH). ^{13}C NMR (DMSO-d_6) δ (ppm.): 6.8 (Sn-CH_3), 30.7 (NH-CH_3), 112.6, 113.7, 115.6, 118.6, 140.7, 153.9 (Ar-C), 155.0 (C=N), 177.2 (S-C-S). ^{119}Sn NMR (DMSO-d_6) δ (ppm.): -123.

*Tin(IV) compound of 2-(2,3-dihydroxybenzylidene)-N-methylhydrazinecarbothioamide (**10**)*

Compound **10** was prepared following the same procedure as described for **5**, using **1** (0.46 g, 2 mmol). Orange solid. Yield: 79 %. Melting point: >300 °C. Analysis calculated for $C_{18}H_{18}N_6O_4S_2Sn$: C, 38.25; H, 3.21; N, 14.87. Found: C, 36.62; H, 2.92; N, 14.21 %. FT-IR (ATR, cm^{-1}): 1585 *v*(C=N), 993 *v*(N-N), 951 *v*(C=S). ^{1}H NMR (DMSO-d_6) δ (ppm.): 2.83 (s, 3H, N-CH_3), 6.65-7.52 (m, 6H, Ar-H), 8.34 (s, 1H, OH), 8.77 (s, 1H, CH), 11.27 (s, 1H, NH).

^{13}C NMR (DMSO-d_6) δ (ppm.): 30.6 (NH-CH_3), 113.8, 114.3, 116.7, 118.9, 140.0. 150.1 (Ar-C), 150.6 (C=N), 177.5 (S-C-S). ^{119}Sn NMR (DMSO-d_6) δ (ppm.): 519.

*2.3.4. General procedure for the syntheses of tin(IV) compounds derived from **2***

Compound **2** (0.30 g, 1 mmol) was dissolved in methanol (100 cm^3) and Et_3N (0.28 cm^3, 2 mmol) was added dropwise to the solution of **2**. The mixture was heated (40 °C) for about 2 hours until the solution was reduced by half. Next 1 mmol of the tin precursor (Ph_2SnCl_2 (0.34 g)/Me_2SnCl_2 (0.22 g)/ $SnCl_2$ (0.19 g)) was added to the mixture. The mixture was refluxed under nitrogen for about 2 hours and filtered while hot to remove the triethylamine salt and the filtrate was kept at room temperature until a bright yellow product formed.

*Diphenyltin(IV) compound of 2-(2-hydroxy-3-methoxybenzylidene)-N-phenylhydrazine carbothioamide (**11**)*

Yellow crystals. Yield: 73 %. Melting point: 205-207 °C. Analysis calculated for $C_{27}H_{23}N_3O_2SSn$: C, 56.67; H, 4.05; N, 7.34. Found: C, 57.53; H, 4.26; N, 7.87%. FT-IR (ATR, cm^{-1}): 3331 *ν*(N-H), 1586 *ν*(C=N), 1075 *ν*(N-N), 832 *ν*(C=S). ^{1}H NMR ($CDCl_3$) δ (ppm.): 3.96 (s, 3H, O-CH_3), 7.99 (s, 1H, CH), 6.69-7.56 (m, 18H, Ar-H), 8.70 (s, 1H, NH). ^{13}C NMR ($CDCl_3$) δ (ppm.): 56.7 (O-CH_3), 115.2, 116.2, 116.9, 119.4, 120.7, 123.4, 124.1, 125.4, 128.7, 128.9, 130.0, 135.9, 139.3, 142.1, 148.3, 149.7, 151.7 (Ar-C), 162.5 (C=N), 164.8 (S-C-S). ^{119}Sn NMR ($CDCl_3$) δ (ppm.): -242.

*Dimethyltin(IV) compound of 2-(2-hydroxy-3-methoxybenzylidene)-N-phenylhydrazine carbothioamide (**12**)*

Yellow crystals. Yield: 64 %. Melting point: 176-179 °C. Analysis calculated for $C_{17}H_{19}N_3O_2SSn$: C, 45.56; H, 4.27; N, 9.38. Found: C, 45.86; H, 4.40; N, 7.08%. FT-IR (ATR, cm^{-1}): 3294 *ν*(N-H), 1577 *ν*(C=N), 1059 *ν*(N-N), 824 *ν*(C=S). ^{1}H NMR ($CDCl_3$) δ (ppm.): 3.85 (s, 3H, O-CH_3), 7.53 (s, 1H, CH), 6.69-7.32 (m, 8H, Ar-H), 8.65 (s, 1H, NH). ^{13}C NMR ($CDCl_3$) δ (ppm.): 6.5 (Sn-CH_3), 56.2 (O-CH_3), 115.3, 116.6, 116.7, 120.5, 123.3, 125.4, 128.9, 139.4, 151.3, 156.8 (Ar-C), 162.5 (C=N), 163.9 (S-C-S). ^{119}Sn NMR ($CDCl_3$) δ (ppm.): -115.

*Tin(IV) compound of 2-(2-hydroxy-3-methoxybenzylidene)-N-phenylhydrazine carbothioamide (**13**)*

Compound **13** was prepared following the same procedure as described for **11**, using **2** (0.60 g, 2 mmol). Yellow solid. Yield: 50 %. Melting point: 293-294 °C. Analysis calculated for $C_{30}H_{26}N_6O_4S_2Sn$: C, 50.23; H, 3.65; N, 11.71. Found: C, 49.85; H, 3.73; N, 11.60%. FT-IR (ATR, cm^{-1}): 3303 *ν*(N-H), 1581 *ν*(C=N), 1063 *ν*(N-N), 824 *ν*(C=S). ^{1}H NMR (DMSO-d_6) δ (ppm.): 3.58 (s, 6H, O-CH_3), 9.08 (s, 2H, CH), 6.80-7.73 (m, 16H, Ar-H), 9.70 (s, 2H, NH). ^{13}C NMR (DMSO-d_6) δ (ppm.): 56.4 (O-CH_3), 117.9, 118.2, 121.0, 123.4, 126.8, 129.2, 140.4, 151.4, 154.8 (Ar-C), 160.3 (C=N), 162.2 (S-C-S). ^{119}Sn NMR (DMSO-d_6) δ (ppm.): -451.

*2.3.5. General procedure for the synthesis of tin(IV) compounds derived from **4***

Compound **4** (0.29 g, 0.001 mol) was dissolved in methanol (100 cm^3) and KOH (0.11 g, 2 mmol) was added dropwise to the solution of **4**. The mixture was refluxed for about 30 minutes, whereupon the color changed from light yellow to orange. Next 1 mmol of the tin precursor (Ph_2SnCl_2 (0.34 g)/Me_2SnCl_2 (0.22 g)/$SnCl_2$ (0.19 g)) was added to the mixture. The mixture was refluxed for 6 hours and filtered while hot to remove the triethylamine salt and the filtrate was kept at room temperature until the product, an orange precipitate, formed.

*Diphenyltin(IV) compound of 2-(2,3-dihydroxybenzylidene)-N-phenylhydrazine carbothioamide (**14**)*

Orange solid. Yield: 71 %. Melting point: 133-137 °C. Analysis calculated for $C_{26}H_{21}N_3O_2SSn$: C, 55.94; H, 3.79; N, 7.53. Found: C, 56.30; H, 3.99; N, 7.42%. FT-IR (ATR, cm^{-1}): 1587 *ν*(C=N), 998 *ν*(N-N), 957 *ν*(S-C-S). ^{1}H NMR (DMSO-d_6) δ (ppm.): 6.57-9.52 (m, 18H, Ar-H), 9.87 (s, 1H, CH), 11.69 (s, 1H, NH). ^{13}C NMR (DMSO-d_6) δ (ppm.): 120.5, 120.7, 125.4, 125.5, 125.6, 125.7, 128.5, 128.6, 128.7, 128.8, 128.9, 129.0, 129.1, 129.5, 134.6, 135.2, 135.5, 136.3, 136.4, 136.7, 139.7 (Ar-C), 148.8 (C=N), 175.2 (S-C-S). ^{119}Sn NMR (DMSO-d_6) δ (ppm.): -328.

*Dimethyltin(IV) compound of 2-(2,3-dihydroxybenzylidene)-N-phenylhydrazine carbothioamide (**15**)*

Orange solid. Yield: 42 %. Melting point: 153-156 °C. Analysis calculated for $C_{16}H_{17}N_3O_2SSn$: C, 44.27; H, 3.95; N, 9.68. Found: C, 44.32; H, 3.72; N, 9.90%. FT-IR (ATR, cm^{-1}): 1575 *ν*(C=N), 1001 *ν*(N-N), 917 *ν*(S-C-S). ^{1}H NMR (DMSO-d_6) δ (ppm.): 0.63 (s, 6H, CH_3), 8.51 (s, 1H, CH), 6.33-7.75 (m, 8H, Ar-H), 9.84 (s, 1H, OH). ^{13}C NMR

(DMSO-d_6) δ (ppm.): 7.1 (Sn-CH_3), 110.2, 114.7, 128.3, 128.4, 128.7, 128.8, 135.3, 152.1, 152.7, 153.6 (Ar-C), 153.8 (C=N), 167.5 (S-C-S). ^{119}Sn NMR (DMSO-d_6) δ (ppm.): -103.

*Tin(IV) compound of 2-(2,3-dihydroxybenzylidene)-N-phenylhydrazinecarbothioamide (**16**)*

Compound **16** was prepared following the same procedure as described for **14**, using **4** (0.58 g, 2 mmol). Orange solid. Yield: 48 %. Melting point: >300 °C. Analysis calculated for $C_{28}H_{22}N_6O_4S_2Sn$: C, 48.78; H, 3.22; N, 12.19. Found: C, 48.30; H, 2.97; N, 12.52 %. FT-IR (ATR, cm^{-1}): 1588 *v*(C=N), 1001 *v*(N-N), 939 *v*(S-C-S). ^{1}H NMR (DMSO-d_6) δ (ppm.): 6.66-7.55 (m, 16H, Ar-H), 8.48 (s, 2H), 10.00 (s, 2H, CH), 11.74 (s, 2H, NH). ^{13}C NMR (DMSO-d_6) δ (ppm.): 117.1, 119.5, 121.2, 125.6, 125.7, 125.9, 126.0, 128.4, 128.5, 128.5, 139.6 (Ar-C), 145.9, 146.0 (C=N), 175.7, 176.1 (S-C-S). ^{119}Sn NMR (DMSO-d_6) δ (ppm.): -541.

2.4. X-ray structure determination

Intensity data for light-yellow crystals of **11′** (0.05 × 0.08 × 0.12 mm) and **12** (0.07 × 0.13 × 0.18 mm) a were measured at 150 K on an Oxford Diffraction Gemini Eos CCD diffractometer (Rigaku Oxford Diffraction, United Kingdom) fitted with Mo Kα radiation (λ = 0.71073 Å). Data reduction and empirical absorption corrections, based on a multi-scan technique, were applied [31]. The structures were solved by direct methods [32] and refined on F^2 with anisotropic displacement parameters, with C-bound H atoms in the riding model approximation [33]. The oxygen- and nitrogen-bound H atoms were refined with distance restraints of O–H = 0.84 ± 0.01 Å and N–H = 0.88 ± 0.01 Å, respectively. A weighting scheme of the form $w = 1/[\sigma^2(F_o^2) + (aP)^2]$, where $P = (F_o^2 + 2F_c^2)/3$, was introduced in each case; for **11′** a = 0.033 and for **12** a = 0.022. The absolute structure of **12** was determined based on differences in Friedel pairs included in the data set. The molecular structure diagrams were generated at the 70% probability level by ORTEP for Windows [34] and the packing diagrams were prepared with DIAMOND [35]. Additional analysis was conducted with PLATON [36].

Crystal data for **11′**: $C_{27}H_{23}N_3O_2SSn$, 0.5($C_{16}H_{16}N_2O_4$), M = 722.43, monoclinic, $P2_1/c$, a = 14.7977(5), b = 13.0726(4), c = 17.0997(6) Å, β = 105.421(3)°, V = 3188.75(19) Å^3, Z = 4, D_x = 1.505 g cm^{-3}, F(000) = 1468 and μ = 0.912 mm^{-1}. No. reflections measured = 14861 (θ_{max} = 29.4°), no. independent reflections = 7337, no. reflections with $I \geq 2\sigma(I)$ = 5378, R (obs. data) = 0.041 and wR_2 (all data) = 0.087. CCDC deposition number: 1975499.

Crystal data for **12**: $C_{17}H_{19}N_3O_2SSn$, M = 448.10, orthorhombic, $P2_12_12_1$, a = 7.7253(2), b = 12.4692(3), c = 18.2692(5) Å, V = 1759.84(8) Å^3, Z = 4, D_x = 1.691 g cm^{-3}, F(000) = 896 and μ = 1.585 mm^{-1}. No. reflections measured = 11201 (θ_{max} = 29.3°), no. independent reflections = 4191, no. reflections $I \geq 2\sigma(I)$ = 3900, R (obs. data) = 0.030 and wR_2 (all data) = 0.096. CCDC deposition number: 1975500.

2.5. Density Functional Theory (DFT) calculations

DFT calculations were performed using Gaussian09 (Gaussian Inc., Wallingford, CT, USA) [37] and Gaussview5 (Semichem, Inc., Shawnee Mission, KS, USA) [38] software. The molecular structures and geometries of the Schiff bases and tin(IV) compounds were fully optimized using the DFT method with the B3LYP [39,40] hybrid exchange correlation functional, the LanL2DZ pseudopotential on Sn [41–43] and 6-311G(*d*,*p*) Pople basis set for all other atoms. The initial single crystal X-ray molecular structures and geometries for the tin compounds in **11** and **12** were used for the DFT calculations, using the same functional and basis set. Vibrational frequencies were scaled using a scaling factor of 0.9682 [44]. The electronic stabilities of the optimized geometries were computed using the time-dependent density functional theory (TD-DFT) formalism [45,46] and included solvation effects (DMSO) *via* the polarizable continuum method (PCM) [47–49], using the same basis set. These DFT calculations were performed in the same way as reported in a previous publication [25].

2.6. In vitro cytotoxic assay

The cytotoxicity of the tin(IV) compounds against HT29 (colon), U87 and SJ-G2 (glioblastoma), MCF-7 (breast), A2780 (ovarian), H460 (lung), A431 (skin), DU145 (prostate), BE2-C (neuroblastoma) and MIA (pancreas) cell lines, and one normal breast cell line, MCF-10A, were measured using an MTT assay, by the same method as previously reported [25,50,51].

Cell culture and stock solutions. Stock solutions were prepared as follows and stored at −20 °C: The synthesised compounds and cisplatin were stored as 10 mM solutions in DMSO and saline solution respectively. All cell lines were cultured in a humidified atmosphere 5% CO_2 at 37 °C. The cancer cell lines were maintained in Dulbecco's modified Eagle's medium

(DMEM) (Trace Biosciences) supplemented with 10% fetal bovine serum, 10 mM sodium bicarbonate, penicillin (100 IU/mL), streptomycin (100 μg/mL) and glutamine (4 mM). The normal cell line, MCF-10A, was cultured in DMEM:F12 (1:1) cell culture media, 5% heat inactivated horse serum, supplemented with penicillin (50 IU/mL), streptomycin (50 μg/mL), 20mM Hepes, L-glutamine (2 mM), epidermal growth factor (20 ng/mL), hydrocortisone (500 ng/mL), cholera toxin (100 ng/mL) and insulin (10 μg/mL).

In vitro growth inhibition assay. Cells in logarithmic growth were transferred to 96-well plates. The cytotoxicity was determined by plating cells in duplicate in 100 μL medium at a density of 2500–4000 cells/well. On day 0 (24 h after plating), when the cells were in logarithmic growth, 100 μL medium, with or without the test agent, were added to each well. After 72 h drug exposure, the growth inhibitory effects were evaluated using an MTT (3-[4,5-dimethylthiazol-2-yl]-2,5-diphenyltetrazolium bromide) assay and the absorbance was read at 540 nm. Percentage growth inhibition was determined at a fixed drug concentration of 25 μM. A value of 100% was indicative of complete cell growth inhibition. Those analogs showing appreciable percentage growth inhibition underwent further dose response analysis, allowing for the calculation of a GI_{50} value. This value is the drug concentration at which cell growth is 50% inhibited based on the difference between the optical density values on day 0 and those at the end of the drug exposure [52,53].

3. Results and discussion

3.1. Synthesis

The synthetic pathways for the Schiff bases (**1-4**) and their tin(IV) compounds (**5-16**) are indicated in Schemes 1 and 2. The Schiff bases were synthesized by the condensation reaction between 2-hydroxy-3-methoxybenzaldehyde/2,3-dihydroxybenzaldehyde and the corresponding thiosemicarbazide (4-methyl-3-thiosemicarbazide and 4-phenyl-3-thiosemicarbazide) in alcoholic solution, which was as previously reported [27,54,55]. The Schiff bases were then reacted with Ph_2SnCl_2, Me_2SnCl_2 and $SnCl_2$ separately, in the presence of potassium hydroxide (KOH)/triethyamine (Et_3N) by conventional methods or under reflux. The isolated yellow or orange colored tin(IV) compounds were obtained in acceptable yields (31-79%), however, some were produced in low yields due to their instability at room temperature. The tin(IV) compounds were soluble in most organic

solvents, especially dimethylsulfoxide (DMSO) and dimethylformamide (DMF). The molar conductance values of the compounds were in the range 0.88-7.85 Ω^{-1} cm^2 mol^{-1}, which was well below 25 Ω^{-1} cm^2 mol^{-1}, indicating that all the compounds were non-electrolytic in nature. This means that no counter ions were present in the outer coordination sphere [56].

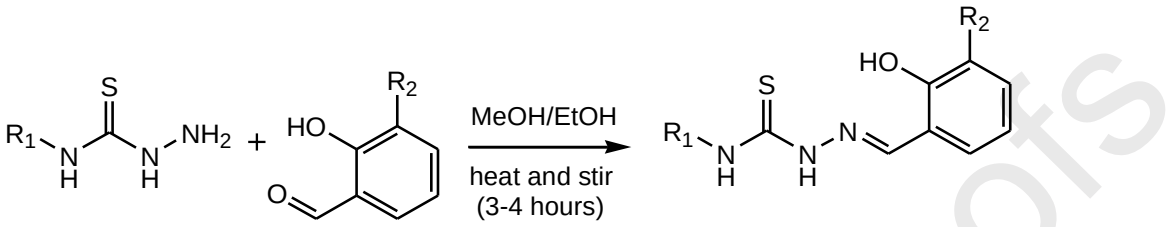

Scheme 1. Synthetic pathway to the thiosemicarbazone Schiff bases **1**-**4**.

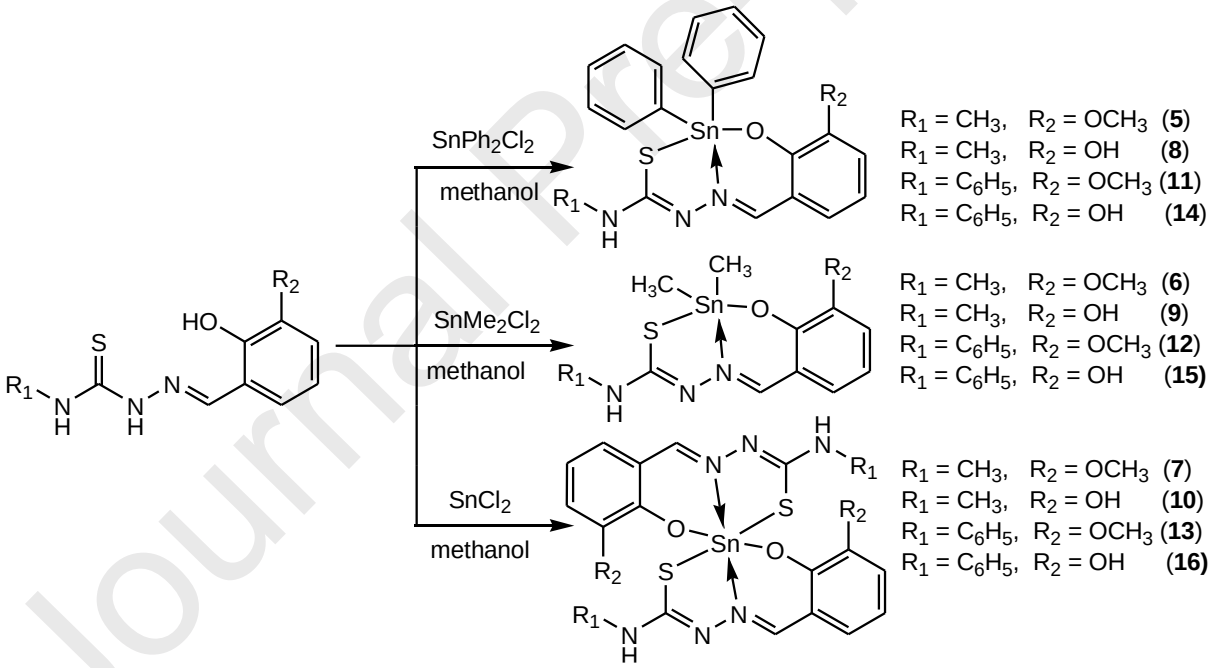

Scheme 2. Synthetic pathway of the thiosemicarbazone Schiff bases to the tin(IV) compounds (**5**-**16**)

3.2. Spectroscopic and spectrometric data

3.2.1. FTIR analysis

The experimental and calculated frequencies in the infrared spectra of the thiosemicarbazone Schiff bases (**1**-**4**) and their tin(IV) compounds (**5-16**) were determined in the range 4000-280 cm^{-1} and 4000-0 cm^{-1}, respectively. Important infrared vibrations and their assignments are summarized in Table S1 for both experimental and calculated frequencies. The calculated frequencies were employed to assign prominent peaks with maximum accuracy, which resulted in excellent correlation with the experimental data (Figure S1). In the spectra of **1** and **2**, the *ν*(OH) band was not observed, which suggested that the *ν*(OH) band overlapped with the *ν*(N-H) band due to hydrogen bonding (NH...OH) between the two groups [57,58]. The *ν*(OH) band was observed in the calculated spectra because they were generated from gas phase structures, while the experimental spectra were analyzed in the solid state where the compounds are in a more concentrated form, resulting in either intermolecular and/or intramolecular hydrogen bonding, similar to that observed in structurally-related Schiff bases [23,59,60]. Conversely, the *ν*(OH) band was observed in the spectra of **3** and **4**, which were comparable to previous literature [23]. As a result, the loss of *ν*(OH) upon complexation was difficult to assign by FTIR alone, due to the intra- and intermolecular hydrogen bonding between the molecules. The *ν*(N-H) band of the thiosemicarbazone Schiff bases disappeared upon complexation due to the deprotonation of the NH group and the involvement of the resulting nitrogen atom in coordination to the Sn center. Furthermore, the IR spectra of **1**, **2**, **3** and **4** exhibited a strong intensity band due to the presence of $\nu(C{=}N)_{azomethine}$ at 1610, 1609, 1601 and 1597 cm^{-1}, respectively. This band shifted to lower frequencies in the spectra of the tin(IV) compounds, suggesting coordination to the tin center *via* the azomethine nitrogen atom. Other than that, the *ν*(C=S) and *ν*(N-N) absorptions shifted to lower frequencies upon complexation, indicating coordination *via* the thiolate sulfur and azomethine nitrogen atoms forming five-membered chelate rings. A small deviation was observed in the vibrational frequencies which can be explained by the fact that the experimental spectra were obtained in the solid state, while the DFT calculations were run in the gas phase.

3.2.2. Multinuclear (^{1}H, ^{13}C and ^{119}Sn) NMR spectral analysis

The ^{1}H and ^{13}C NMR spectra of **1-4** were recorded in DMSO-d_6 solution and **5-16** were recorded in DMSO-d_6/$CDCl_3$ solution at room temperature. The assignments of the relevant signals are compiled in Tables S2 and S3. The ^{1}H NMR spectra of **1-4** showed signals at δ 11.42, 11.78, 11.40 and 11.75 ppm, respectively, which indicated the presence of -NH- protons. These -NH- proton signals were not present in the spectra of the tin(IV) compounds, indicating that the Schiff bases were coordinated to the tin atoms *via* the nitrogen donor atom.

Proton signals appeared at δ 9.18 and 10.02 ppm for **1** and **2** corresponding to the hydroxyl atom, which disappeared in the ^{1}H NMR spectra of the tin(IV) compounds, indicating the coordination of the hydroxyl proton to the tin center [61]. Contrastingly, the two signals for hydroxyl groups at δ 8.37, 8.38 ppm (**3**) and δ 8.96, 9.52 ppm (**4**) disappeared upon complexation, which indicated the presence of intra- and intermolecular hydrogen bonding in the compounds [23,62].

The ^{13}C NMR spectra of **1**, **2**, **3** and **4** showed carbon signals at δ 177.6, 176.1, 178.0 and 176.0 ppm, respectively in the downfield region attributed to -S-C(=S)N. The position of these carbon signals proved that the compounds are predominately thione tautomers, even in DMSO-d_6 solution. The signals shifted to the upfield region in the spectra of the tin(IV) compounds, indicative of the involvement of the -S-C(-S)N moiety in the complexation and decreasing electron density at the carbon atom when the sulfur atom is chelated to the tin atom. The C=N signal was assigned at δ 148.4, 148.6, 146.0 and 146.0 ppm for **1**-**4**, respectively, and appeared downfield as the carbon atom is bonded to electronegative atoms. However, the C=N signals shifted downfield in the spectra of the tin(IV) compounds due to the increasing electron density around the atom upon complexation. The -CH_3- unit of the methoxy group appeared in the upfield region at δ 56.4 (**1**) and 56.3 ppm (**2**). A similar carbon signal was observed for the -CH_3- unit of the methoxy group in the spectra of the tin(IV) compounds, indicating that the methoxy group does not coordinate to the tin atom.

The ^{119}Sn NMR data was used to predict the geometry of the tin-containing compounds. The ^{119}Sn NMR spectra of compounds **5**-**16** were evaluated in DMSO/$CDCl_3$ solutions at room temperature using $SnCl_4$ (δ = -150 ppm) as an external standard. The ^{119}Sn chemical shift strongly depends on the alkyl/aryl group attached to the tin atom and the electronegativity of the ligand coordinated to the tin atom, as well as the temperature employed in the experiments. Theoretically, as the coordination number increases, the ^{119}Sn chemical shift moves towards the shielding region [63]**.** The spectra showed one sharp signal which indicated that the tin(IV) compounds had only a single tin atom species. The ^{119}Sn NMR values of the penta-coordinated diphenyl- (**5**, **8**, **11** and **14**) and dimethyltin(IV) (**6**, **9**, **12** and **15**) compounds fell in the ranges δ -227 to -328 and -103 to -154 ppm, respectively, similar to that reported previously for diphenyl- and dimethyltin(IV) compounds [64–67]. The ^{119}Sn NMR values of the hexa-coordinated tin(IV) compounds (**7**, **10**, **13** and **16**) were observed in the range δ -354 to -541 ppm. The ^{119}Sn NMR values of compounds **8**, **10**, **14**, and **16** were

more negative due to the presence of hydroxyl groups at the *meta* position, which are more electronegative than the methoxy groups [68].

3.2.3. Mass spectrometric analysis

Mass spectral data for **1-4** were recorded in DMSO and were found to be consistent with the proposed formulation of the Schiff bases. The mass spectra displayed prominent peaks at m/z 239, 301, 225, and 287 for Schiff bases **1-4**, respectively, which correspond to the $[C_{10}H_{13}N_3O_2S]^+$, $[C_{15}H_{15}N_3O_2S]^+$, $[C_9H_{11}N_3O_2S]^+$ and $[C_{14}H_{13}N_3O_2S]^+$ ions; the mass spectra for **1-4** are supplied in Figure S2.

3.2.4 Electronic spectral analysis

The experimental and calculated electronic data of compounds **1-16** in DMSO are tabulated in Table S4. The prominent experimental electronic absorptions for **1-4** were observed in the range 328-334 nm, which were best correlated with the calculated absorptions by B3LYP in the range 317-330 nm. The frontier molecular orbitals of compounds **1-16** are shown in Figure S3, where the figure illustrates the excitation of electrons from the HOMO of non-bonding electrons at sulfur and nitrogen atoms that were excited to the LUMO, which is largely centered on the thiosemicarbazone backbone, 2,3-dihydroxy phenyl ring and as well as the oxygen atom attached to the phenyl ring. Thus, this supported the transition of electrons from n→π* and π→π* of the Schiff bases. For the tin(IV) compounds (**5-16**), the HOMOs are largely centered on the thiosemicarbazone Schiff base, whereas the LUMOs are centered on the entire thiosemicarbazone Schiff base except the methyl or phenyl groups attached to the nitrogen atom, thiolate sulfur and oxygen atoms attached to the phenyl ring.

*3.3. X-ray structure crystallography of **11′** and **12***

3.3.1. Molecular structures

The crystallographic asymmetric unit of **11′** comprises a molecule of $Ph_2Sn(L^2)$ (**11**) and half a molecule of 3-methoxysalicylaldehyde azine, with the molecular structures of each shown in Figure 2. The presence of the azine molecule in **11′** presumably arises from the prolonged standing of the acetonitrile:methanol (1:1) solution during the crystallization of an authenticated sample of **11**, which resulted in partial decomposition of **11** and subsequent condensation of hydrazine and *o*-vanillin to form the azine. The tin center in **11′** is coordinated by two *ipso*-carbon atoms of the phenyl substituents as well as the imine-N,

phenoxide-O and thiolate-S atoms derived from the di-negative, tridentate Schiff base ligand. The resulting coordination geometry defined by the C_2NOS donor set is highly distorted from an ideal trigonal-bipyramidal geometry. This is quantified by the value of $\tau = 0.60$, which lies between the extreme values of 1.0 and 0.0 for the ideal geometries of trigonal-bipyramidal and square pyramidal [69]. The angle closest to being *trans* is the S1–Sn–O1 angle of 161.81(7)°, with the next widest angle of 125.85(10)° being for N2–Sn–C16. Selected geometric parameters are collated in the caption to Figure 2. While the crystal structure of L^2H_2 is not available for comparison, that of the 4-methoxy analogue, L^5H_2, is available [70]. In L^2H_2 the formally C1=S1 thione bond is 1.6769(14) Å, which is considerably shorter than the C1–S1 bond length of 1.748(3) Å in **11′**. The other parameters of interest relate to the shortening of the C1–N1 bond in **11′** to 1.290(4) Å compared with 1.3441(17) Å in L^5H_2 and the small increase in the formally imine-C2=N2 bond to 1.309(4) compared with 1.2798(18) Å in L^5H_2 [70].

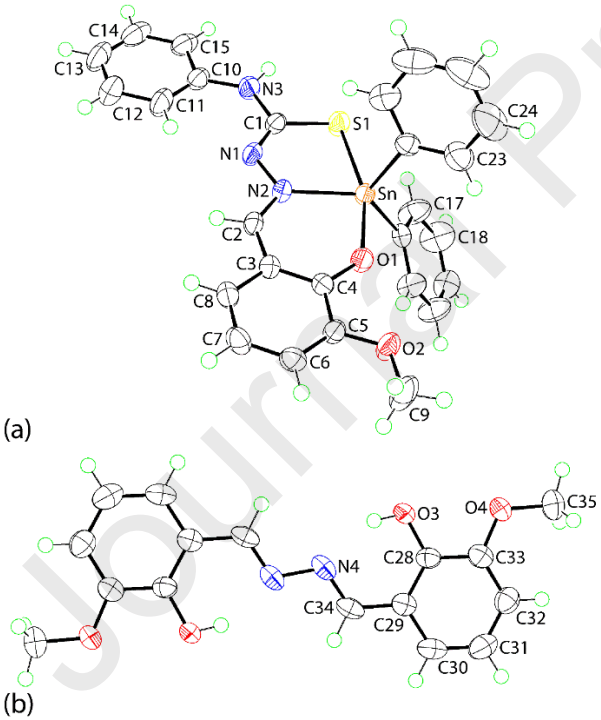

Figure 2. The molecular structure of the constituents of **11′** showing the atom-labelling scheme and 70% probability displacement ellipsoids. The 3-methoxysalicylaldehyde azine molecule in (b) is disposed about a crystallographic center of inversion with unlabelled atoms related by the symmetry operation *-x*, 3-*y*, *-z*. Selected geometric parameters: Sn–S1 =

2.5475(8), Sn–O1 = 2.0853(19), Sn–N2 = 2.176(3), S1–C1 = 1.748(3), N1–N2 = 1.394(3), N1–C1 = 1.290(4), and N2–C2 = 1.309(4) Å. Details of the intramolecular hydroxy-O–H···N(azine) hydrogen bond: H3o···N4 = 1.84(3) Å, O3···N4 = 2.598(4) Å with the angle at H3o = 150(3)°.

The major distortions in the coordination geometry about the tin atom in **11′** can be traced to the formation of five- (Sn,S1,N1,N2,C1) and six-membered (Sn,O1,N2,C2-C4) chelate rings by the tridentate ligand, resulting in tight S1–Sn–N2 [77.76(6)°] and O1–Sn–N2 [84.62(9)°] chelate angles. Each chelate ring is essentially planar, as seen in the values of the root mean square (r.m.s.) deviations of 0.047 Å [maximum deviation = 0.035(3) Å for the C1 atom] and 0.025 Å [0.026(3) Å for C3] for the five- and six-membered rings, respectively. The dihedral angle formed between the chelate rings is 2.81(9)°, indicating these rings are coplanar, and the dihedral angle between the terminal rings is 5.36(15)°, indicating the Schiff base di-anion is essentially planar.

The second constituent of **11′** is a half a molecule of 3-methoxysalicylaldehyde azine, with the full molecule being generated by the application of crystallographic inversion symmetry. The molecule is constructed about a central azine-N4–N4^{i} bond [1.401(5) Å for symmetry operation (i) -*x*, 3-*y*, -*z*] and features intramolecular hydroxy-O–H···N(azine) hydrogen bonds which close *S*(6) loops; see Figure 2 for details. The crystal structure determination of this molecule has been reported several times and in two polymorphs. A form is known [71] where the molecule is disposed about a center of inversion [N–N = 1.4025(14) Å], as in **11′**, as well as a non-symmetric version [N–N = 1.402(5) Å], which approximates a centrosymmetric conformation [72].

To a first approximation, the molecular structure of **12**, Figure 3, mirrors that found for the diphenyltin compound in **11′**. Thus, a similar coordination mode is adopted by the L^1 di-anion, but in this case, based on a value of $\tau = 0.0$ [69], the coordination geometry is distorted square pyramidal. In this description, the Sn atom lies 0.6358(18) Å out of the basal plane defined by the S1, O1, N2 and C16 atoms [r.m.s. deviation = 0.0078 Å] in the direction of the axially-bound C17 atom. This arises as the two widest angles, that is S1–Sn–O1 [145.67(9)°] and N2–Sn–C16 [145.45(15)°] are virtually identical. The Sn-S1 [2.5475(8)] and Sn-N2 [2.257(3)] bond lengths are, respectively, approximately 0.05 Å shorter and 0.08 Å longer in **12** than the equivalent bonds in **11′**, while the Sn-O1 bond lengths remain the same.

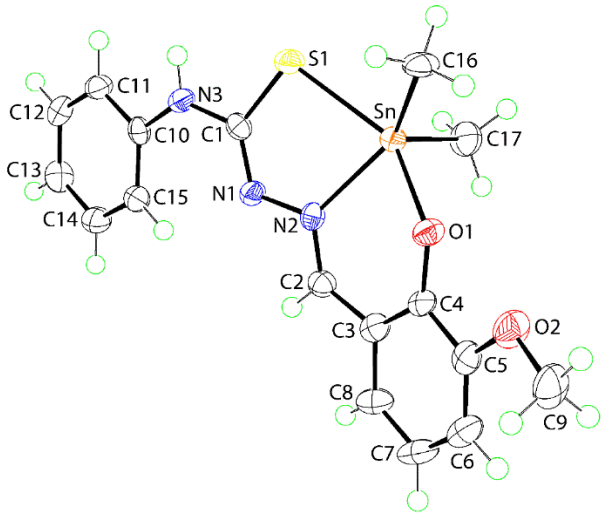

Figure 3. The molecular structure of the constituents of **12** showing atom-labelling scheme and 70% probability displacement ellipsoids. Selected interatomic parameters: Sn–S1 = 2.4982(12), Sn–O1 2.085(3), Sn–N2 = 2.257(3), S1–C1 = 1.751(4), N1–N2 = 1.396(5), N1–C1 = 1.306(5) and N2–C2 = 1.288(5) Å.

The five- and six-membered chelate rings in **12** exhibit r.m.s. deviations of 0.080 Å [maximum deviation = 0.071(3) Å for the N2 atom] and 0.200 Å [0.189(1) Å for Sn], suggesting deviations from planarity. Indeed, the five- and six-membered rings may each be described as having an envelope conformation where, for the smaller ring, the Sn atom lies 0.248(6) Å out of the plane defined by the remaining four atoms [r.m.s. deviation = 0.0056 Å]. The envelope is more pronounced for the larger ring, with the Sn atom 0.612(5) Å above the plane [r.m.s. deviation = 0.0229 Å]. The dihedral angle between the chelate rings is 17.88(12)°, but this reduces to 12.1(2)° when the angle between the planar regions is computed. The dihedral angle between the outer rings is 6.2(2)°.

Thus far, no specific mention of the tin-bound substituents in **11′** and **12** has been made. The Sn–C bond lengths in **11′** are equivalent at 2 × 2.134(3) and, in turn, these are experimentally equivalent to those in **12**, that is, 2.134(4) Å [Sn–C16] and 2.128(4) Å [Sn–C17]. A difference is seen in the C–Sn–C angles, however. Thus, in **11′**, this angle is 121.46(12)° which is significantly wider than the equivalent angle of 114.82(18)° in **12**. This disparity is

emphasized in the overlay diagram shown in Figure 4, as are the differences in the relative orientations of the L^2 di-anions.

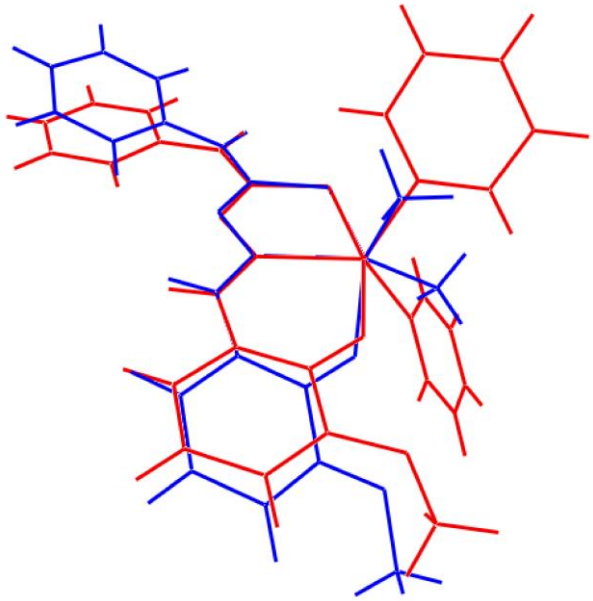

Figure 4. Overlay diagram of the $R_2Sn(L^2)$ molecules in **11′** (R = Ph; red image) and inverted-**12** (R = Me; blue image), whereby the five-membered rings are coincident.

3.3.2. Supramolecular structures

The most notable aspect of the molecular packing of **11′** is the formation of eight-membered $\{\cdots HNCS\}_2$ synthons through the agency of amine-N–H$\cdots$S(thiolate) hydrogen bonds between centrosymmetrically related $Ph_2Sn(L^2)$ molecules, Figure 5(a). Additional interactions between molecules of note are of the type π(chelate ring)$\cdots$π(oxidobenzylidene) stacking, as illustrated in Figure 5(b). Such interactions are increasingly being recognized as being important in providing points of contact in coordination chemistry [73] and computational chemistry indicates these provide energies of stabilization greater than conventional π-stacking interactions between organic residues [74]. The dimeric aggregates are connected into a supramolecular layer in the *ab*-plane *via* L^1-imine-C–H$\cdots$O(hydroxy) and imine-C–H$\cdots$O(methoxy) interactions, as shown in Figure 5(c). In essence, each 3-methoxysalicylaldehyde azine molecule links four symmetry related $Ph_2Sn(L^2)$ molecules. The layers stack along the *c*-axis direction, being connected by tin-bound-phenyl-C-H$\cdots$π(Sn-

phenyl, oxidobenzylidene) and azine-methoxy-C-H···π(N-phenyl) interactions, to consolidate the three-dimensional architecture, Figure 5(d).

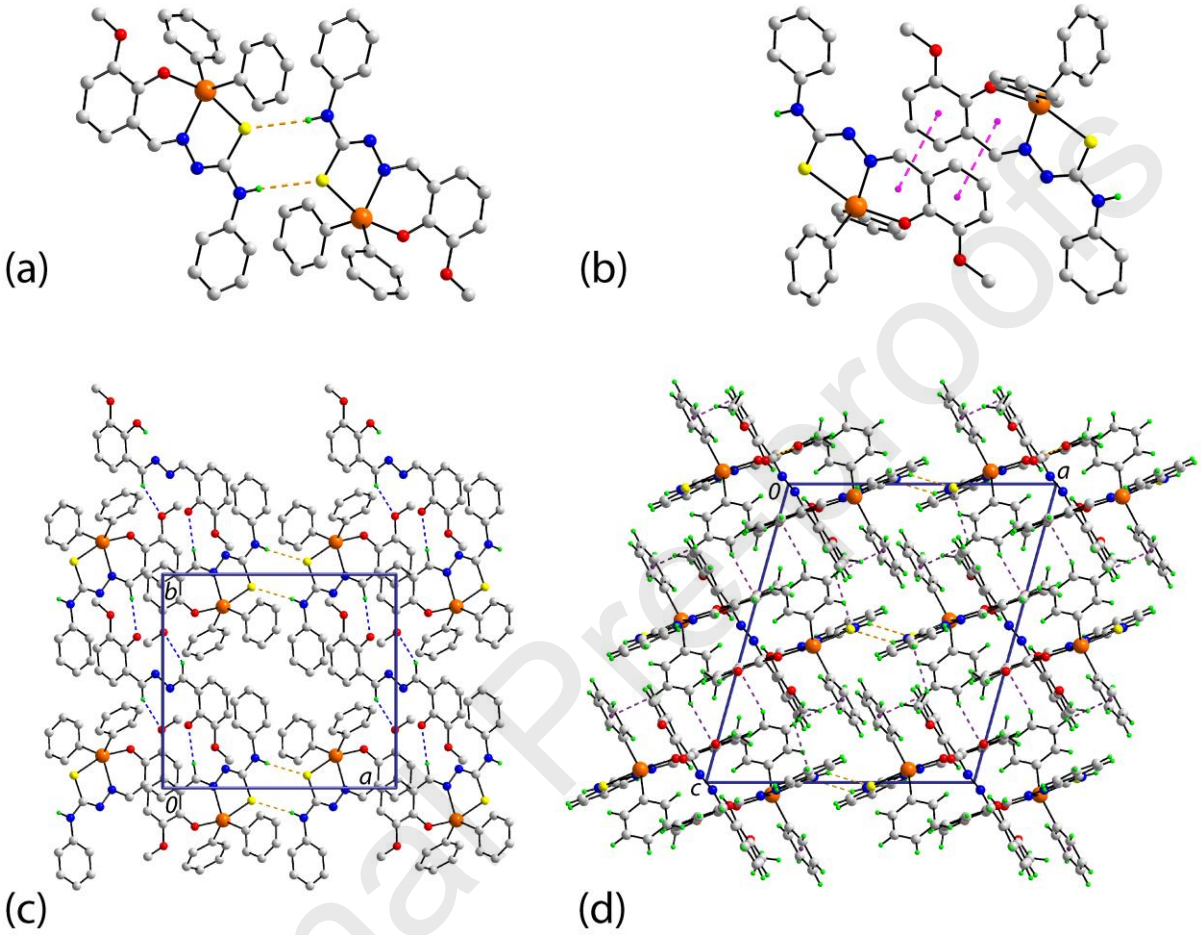

Figure 5. Molecular packing in the crystal of **11′**: (a) a view of the supramolecular dimer sustained by amine-N–H···S(thiolate) hydrogen bonds, shown as orange dashed lines [N3–H3n···S1^{i}: H3n···S1^{i} = 2.60(3) Å, N3···S1^{i} = 3.380(3) Å and angle at H3n= 150(3)° for symmetry operation (i) 1-*x*, 2-*y*, -*z*], (b) a view of the dimer aggregate connected by π(chelate ring)···π(oxidobenzylidene) stacking interactions [Cg(Sn,O1,N2,C1-C3)…Cg(C3-C8)^{ii} = 3.8613(15) Å and angle of inclination = 2.13(11)° for (ii) -*x*, 2-*y*, -*z*] shown as pink dashed lines, (c) supramolecular layer whereby the aggregate shown in (a) is connected by L^{2}-imine-C–H···O(hydroxy) and imine-C–H···O(methoxy) interactions (blue dashed lines) [C2–H2···O3: H2···O3 = 2.40 Å, C2···O3 = 3.336(4) Å and angle at H2 = 168°; C34–H34···O2^{iii}: C34–H34···O2^{iii} = 2.40 Å, C34···O2^{iii} = 3.230(4) Å and angle at H34 = 146° for (iii) *x*, 1+*y*, *z*], and (d) a view of the unit-cell contents in projection down the *b*-axis with C–H···π

interactions shown as purple dashed lines [C18–H18···Cg(C22-C27)^{iv}: H18···Cg(C22-C27)^{iv} = 2.79 Å and angle at H18 = 148°; C19–H19···Cg(C3-C8)^{iv}: H19···Cg(C3-C8)^{iv} = 2.73 Å and angle at H19 = 138°; C35–H35c···Cg(C10-C15)^{v}: H35c···Cg(C10-C15)^{v} = 2.85 Å and angle at H35c = 133° for (iv) *x*, 3/2-*y*, -1/2+*z* and (v) *x*, 5/2-*y*, 1/2+*z*]. In (a)-(c), non-participating hydrogen atoms have been omitted for clarity.

The most prominent aspect of the molecular packing of **12** is the formation of supramolecular chains supported by amine-N–H···O(phenoxide) hydrogen bonding. The chains are aligned along the *a*-axis and have a helical topology, being propagated by 2_1-screw symmetry, Figure 6(a). Further stability to the aforementioned chains is provided by secondary bonding [73,75] of the type Sn···S, well known in organotin chemistry [76]. As detailed in Figure 6(b), the sulfur atom approaches the tin atom from the basal plane to establish a 5+1 coordination geometry; the C17–Sn–S1 angle = 157.48(11)°. When considered in conjunction with the hydrogen bonding, six-membered, {···HNCS···SnO} heterosynthons are established. The chains are assembled into a three-dimensional architecture by amine-N-phenyl-C–H···π(oxidobenzylidene) interactions as each chain forms two donor and two acceptor interactions, Figure 6(c).

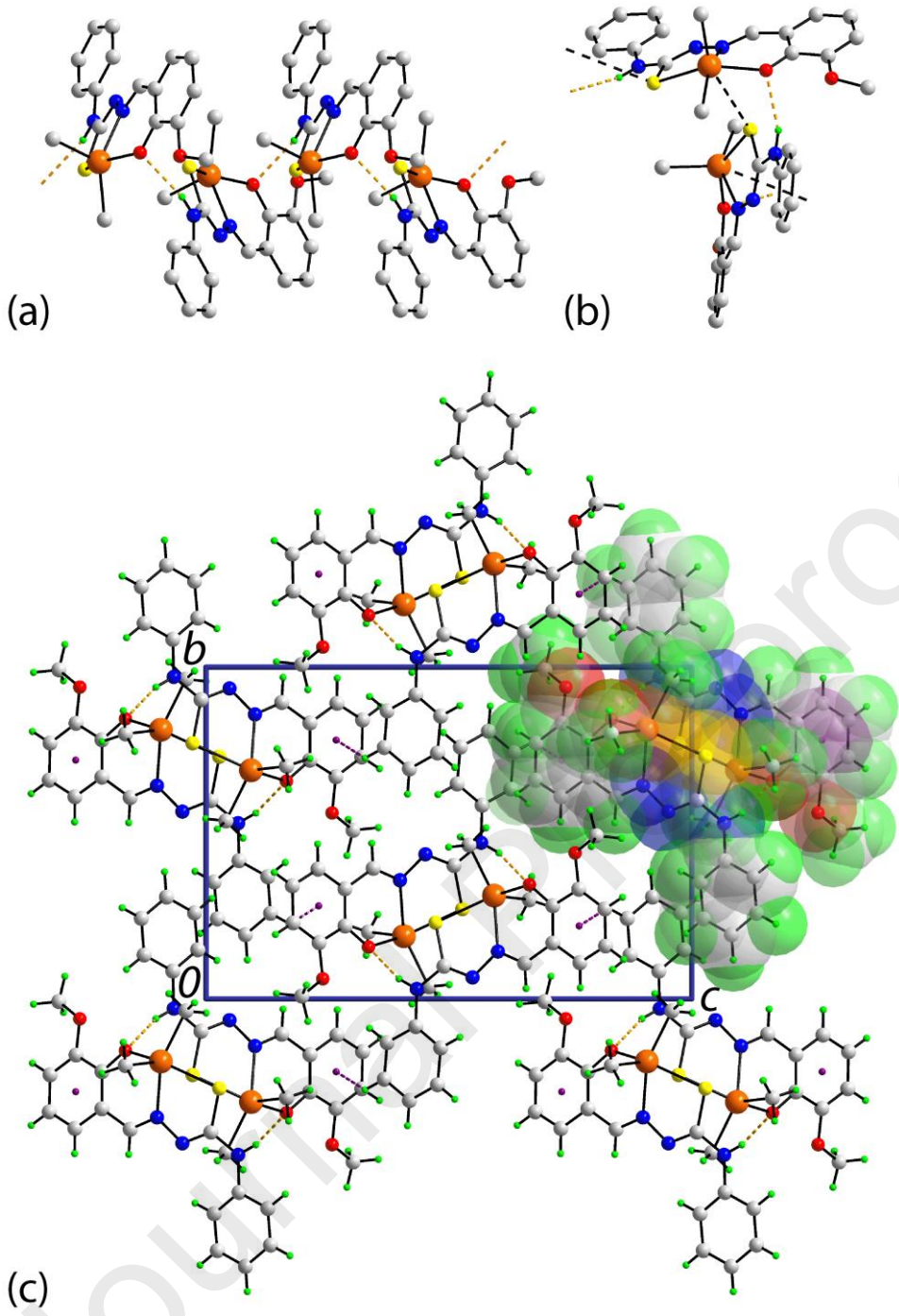

Figure 6. Molecular packing in the crystal of **12**: (a) a view of the supramolecular helical chain sustained by amine-N–H···O(phenoxide) hydrogen bonds, shown as orange dashed lines [N3–H3n···O1^{i}: H3n···O1^{i} = 2.26(4) Å, N3···O1^{i} = 3.089(5) Å and angle at H3n = 160(3)° for symmetry operation (i) 1/2+*x*, 1/2-*y*, 1-*z*], (b) detail of the Sn···S secondary bonding [Sn···S1^{ii} = 3.4928(12) Å for (ii) -1/2+*x*, 1/2-*y*, 1-*z*] within the chain shown in (a) and the resulting six-membered, {···HNCS···SnO} heterosynthon, and (c) a view of the unit-cell contents in a projection down the *a*-axis with one supramolecular chain highlighted in the space-filling

mode. Chains are connected by amine-N-phenyl-C–H···π(oxidobenzylidene) interactions [C12–H12···Cg(C3-C8)^{iii}: H12···Cg3^{iii} = 2.98 Å and angle at H12 = 129° for (iii) 1/2-*x*, 1-*y*, 1/2+*z*] shown as purple dashed lines.

3.4. Cytotoxic activity

Compounds **1**-**16** were screened for their cytotoxicity against a panel of ten cancer cell lines, HT29, U87, SJ-G2, MCF-7, A2780, H460, A431, DU145, BE2-C and MIA, and one normal cell line, MCF-10A (Table 1). However, it was not possible to determine the cytotoxicity values of **7** due to its insolubility in 100% DMSO at 1mM concentration. Cisplatin was used as a positive control to induce cell death. The growth inhibition concentrations of the compounds required to inhibit 50% cell proliferation (GI_{50}) were recorded after 72 hours of cell exposure to the compounds. The stability of the compounds in DMSO and in a mixture of DMSO and H_2O were studied by UV-vis spectroscopic analysis, where the spectra remained unchanged after 72 hours, which indicated that the compounds are stable in both solvent systems.

The cytotoxicity evaluation of the 2-hydroxy-3-methoxybenzyl thiosemicarbazone Schiff base analogues (**1** and **2**) revealed an increase in potency when a methyl substituent was attached to the α-nitrogen atom, where **1** exhibited 10 to 20 times higher anti-proliferative activity as compared that of **2**, **3** and **4** in the panel of cancer cell lines tested. Table 1 shows the high level for the cytotoxic potency of **1** against HT-29, A2780, A431, BE2-C and MIA cell lines. Compound **1** was approximately ~10-100 times more potent than similar synthesized structures, 2-[(1E)-({[(benzylsulfanyl)methanethioyl]amino}-imino)methyl]-6-methoxyphenol (SBOVaH) [25] and 2-hydroxy-5-methoxybenzaldehyde-*N*(4)-methylthiosemicarbazone (H2dmmt) [8] against all the cancer cell lines tested, except for the DU145 cell line. **1** also showed excellent cytotoxicity against the panel of cancer cell lines compared to the reference drug (cisplatin). No obvious cytotoxicity pattern was observed for **2**, which was similar to that of a similar analogue, SBOVaH [25]. In contrast, the 2,3-dihydroxybenzyl thiosemicarbazone Schiff bases (**3** and **4**) showed a different pattern of cytotoxicity, which could be attributed to the phenyl group attached to the α-nitrogen atom, where the phenyl group potentially facilitates binding to biological molecules by π interactions [23]. Compounds **2** and **4** are similar in structure, with the difference being only in the methoxy (**2**) and hydroxyl (**4**) group substituents at the meta position of the benzene

rings. Compound **4** was more active than **2** against all cancer cell lines tested. This was possibly due to the formation of hydrogen bonding interactions of two hydroxyl groups with the active site of the amino acids of various enzymes in the cancer cells [77]. Compound **3** showed poorer cytotoxicity at the 25 µM single point dose evaluation pre-screening and was not selected for further GI_{50} determination as it was considered to be inactive. The cytotoxicity of the Schiff bases was tested using the non-cancerous normal human breast cell line (MCF10A), where **1** showed lower toxicity towards the normal cells, which was evident from its higher GI_{50} value (less active) as compared to the GI_{50} values of most of the cancer cells, except U87, H460 and DU145. Compound **4** also exhibited a higher GI_{50} value against MCF10A than HT29, MCF-7 and A2780. This suggests that **1** and **4** exhibit notable anticancer properties against certain cancer cells as compared to normal cells.

The cytotoxicities of the tin(IV) compounds are comparable to those of related compounds [25] where the diphenyltin(IV) compounds exhibit higher activities against certain cell lines as compared to their Schiff bases and other tin(IV) compounds. In particular, **5** showed higher cytotoxicities than its Schiff base (**1**) towards MCF-7, A2780, H460 and DU145 cells. It was also observed that **5** exhibited a 2.5-fold lower activity than **1** against MIA cells. Compounds **8** and **11** exhibited higher activities than **3** and **2** respectively across all cancer cell lines. In a similar vein, compound **14** was more active than **4** for all cells, except MCF-7, A2780 and H460 cells. The dimethyltin(IV) (**6**, **9**, **12**, and **15**) and tin(IV) (**10**, **13**, and **16**) compounds exhibited no significant differences as compared to their Schiff bases. It can be concluded that the presence of two phenyl groups attached to the tin atom at the center improved the cytotoxicity against all the tested cancer cell lines. The planarity of the aromatic π system makes it available for stacking and provides easier penetration into the double helix of the DNA of cancer cells [78]. Overall, the cytotoxicity data indicate that HT29, MCF-7, A2780, A431, BE2-C and MIA are more sensitive, whereas H460 and DU145 cells are more resistant against the Schiff bases and tin(IV) compounds that were investigated in this study than cisplatin. By comparing the toxicity of the compounds tested, all the tin(IV) compounds (**5-16**) showed lower toxicity for MCF10A cells as the GI_{50} values of MCF10A were higher (less active) than the GI_{50} values of certain cancer cells. However, MCF10A is positive for telomerase reverse transcriptase [79] which is known to be up-regulated in many cancer cells as well. The decrease in cell viability after treatment with the synthesised compounds may be due to the inactivation of this enzyme. The use of MCF10A in this study is to act as a benchmark for the cytotoxicity data obtained [80].

Table 1. *In vitro* cytotoxicity of the tin(IV) compounds (**5-16**) derived from the thiosemicarbazone Schiff bases (**1-4**) against several cell lines, determined by an MTT assay and expressed as GI_{50} values with standard errors. GI_{50} is the concentration at which cell growth is inhibited by 50% 72 hours post-incubation.

Compounds	Growth inhibition concentration, GI_{50} (μM)										
	HT29	U87	MCF-7	A2780	H460	A431	DU145	BE2-C	SJ-G2	MIA	MCF10A
1	**0.09 ± 0.06**	**0.26 ± 0.11**	**0.12 ± 0.08**	**0.037 ± 0.07**	**0.42 ± 0.19**	**0.09 ± 0.06**	nd	**0.03 ± 0.02**	**0.15 ± 0.03**	**0.04 ± 0.02**	0.43 ± 0.29
2	**1.80 ± 0.22**	**3.5 ± 0.40**	**1.9 ± 0.46**	2.0 ± 0.40	1.5 ± 0.27	2.4 ± 0.26	5.1 ± 0.58	**1.0 ± 0.15**	2.5 ± 0.77	**2.1 ± 0.49**	3.3 ± 0.26
3[b]	> 25	> 25	> 25	> 25	> 25	> 25	> 25	> 25	> 25	> 25	> 25
4	**0.29 ± 0.25**	**1.6 ± 0.29**	**0.03 ± 0.01**	**0.041 ± 0.02**	1.0 ± 0.03	**1.4 ± 0.43**	2.1 ± 0.09	**0.7 ± 0.51**	0.8 ± 0.49	**2.5 ± 1.2**	1.5 ± 0.40
5	**0.05 ± 0.02**	**0.14 ± 0.06**	**0.02 ± 0.00**	**0.020 ± 0.00**	**0.22 ± 0.06**	**0.07 ± 0.04**	0.86 ± 0.42	**0.02 ± 0.00**	**0.09 ± 0.04**	**0.11 ± 0.09**	0.15 ± 0.08
6	**0.30 ± 0.05**	6.9 ± 5.1	**0.13 ± 0.03**	**0.20 ± 0.01**	1.3 ± 0.53	**0.35 ± 0.12**	5.0 ± 3.1	**0.15 ± 0.03**	0.48 ± 0.14	**0.15 ± 0.03**	1.0 ± 0.71
7	nd	nd	nd	nd	nd	nd	nd	nd	nd	nd	nd
8	**0.15 ± 0.07**	**0.38 ± 0.10**	**0.10 ± 0.05**	**0.15 ± 0.04**	**0.60 ± 0.10**	**0.49 ± 0.31**	**0.50 ± 0.18**	**0.15 ± 0.04**	0.42 ± 0.18	**0.23 ± 0.07**	0.34 ± 0.15
9	**0.36 ± 0.07**	**2.2 ± 0.33**	**0.22 ± 0.04**	**0.26 ± 0.01**	1.4 ± 0.67	**1.2 ± 0.81**	9.1 ± 3.4	1.5 ± 0.39	1.6 ± 1.2	**0.79 ± 0.36**	3.2 ± 0.33
10	**0.09 ± 0.06**	3.5 ± 3.3	**0.09 ± 0.07**	**0.10 ± 0.08**	>50	nd	25 ± 4.00	**0.15 ± 0.11**	**0.22 ± 0.04**	**0.95 ± 0.21**	0.81 ± 0.60
11	**1.0 ± 0.35**	**0.57 ± 0.13**	**0.31 ± 0.13**	**0.27 ± 0.01**	1.1 ± 0.03	**1.1 ± 0.26**	1.4 ± 0.20	**0.29 ± 0.06**	0.44 ± 0.11	**0.35 ± 0.08**	1.2 ± 0.41
12	**1.8 ± 0.38**	4.8 ± 0.75	**1.6 ± 0.75**	2.1 ± 0.43	2.0 ± 0.18	2.8 ± 0.46	4.8 ± 0.73	**1.1 ± 0.20**	1.3 ± 0.54	**2.0 ± 0.88**	3.2 ± 0.07
13	**1.7 ± 0.74**	3.7 ± 1.3	**2.6 ± 0.48**	2.6 ± 0.37	3.2 ± 0.15	2.6 ± 0.22	5.3 ± 0.67	1.8 ± 0.07	5.0 ± 1.97	**3.3 ± 0.72**	4.4 ± 0.60
14	**0.19 ± 0.05**	**0.32 ± 0.04**	**0.12 ± 0.03**	**0.16 ± 0.04**	**0.53 ± 0.19**	**0.38 ± 0.19**	**0.20 ± 0.05**	**0.13 ± 0.02**	**0.20 ± 0.03**	**0.10 ± 0.02**	0.37 ± 0.08
15	**0.12 ± 0.03**	**0.40 ± 0.07**	**0.10 ± 0.03**	**0.21 ± 0.05**	**0.83 ± 0.37**	**0.27 ± 0.11**	**0.56 ± 0.27**	**0.20 ± 0.05**	**0.23 ± 0.03**	**0.17 ± 0.05**	0.30 ± 0.02
16	**0.18 ± 0.02**	**0.44 ± 0.06**	**0.17 ± 0.08**	**0.27 ± 0.023**	**0.47 ± 0.07**	**0.26 ± 0.03**	**0.42 ± 0.15**	**0.25 ± 0.05**	**0.26 ± 0.02**	**0.23 ± 0.07**	0.34 ± 0.02
Cisplatin	11.0 ± 2.0	4.0 ± 1.0	6.5 ± 0.8	1.0 ± 0.1	0.9 ± 0.2	2.4 ± 0.3	1.2 ± 0.1	1.9 ± 0.2	0.4 ± 0.1	8.0 ± 1.0	nd

[a] 'nd' = not determined; [b] percentage growth inhibition at 25 μM compound concentration

4. Conclusions

A series of twelve tin(IV) compounds derived from four thiosemicarbazone Schiff bases have been synthesized and characterized by physicochemical and spectroscopic techniques, as well as X-ray crystallographic analysis. X-ray crystallography indicated a highly distorted trigonal-bipyramidal coordination geometry for $Ph_2Sn(L^1)$ in **11′** and a distorted square pyramidal geometry for $Me_2Sn(L^1)$ in **12**. An interesting pattern of cytotoxicity was observed where compound **1** was selectively active against HT29, A2780, A431, BE2-C and MIA, while **3** was inactive against all cancer cells. Both were similar in structure, the difference being the methoxy (**1**) and hydroxyl (**3**) substituent at the meta position of the phenyl ring. In contrast, compound **4**, having a hydroxyl group on the phenyl ring, demonstrated greater activity than compound **2** which had a methoxy group. Diphenyltin(IV) compound **5** displayed excellent activity in the range 0.016-0.22 μM against all the cancer cells tested. Overall, the diphenyltin(IV) compounds showed the most promising anticancer potential. Based on findings in this study, the thiosemicarbazone Schiff bases and their tin(IV) compounds have significant anticancer potential and further mechanism of action and *in vivo* studies are required to determine the action of these compounds *in vivo* for a better intracellular understanding.

Appendix A. Supplementary data CCDC 1975499 and 1975500 contains the supplementary crystallographic data for **11'** and **12**. These data can be obtained free of charge via http://www.ccdc.cam.ac.uk/conts/retrieving.html, or from the Cambridge Crystallographic Data Centre, 12 Union Road, Cambridge CB2 1EZ, UK; fax: (+44) 1223-336-033; or e-mail: deposit@ccdc.cam.ac.uk.

Funding: This research was funded by Universiti Putra Malaysia under the Geran Putra IPS (9504600) and Geran Putra IPB (9581001) (UPM) and the Malaysian Fundamental Research Grant Scheme (FRGS No. 01-01-16- 1833FR).

Acknowledgements: We thank the Department of Chemistry, the Molecular Genetics Laboratory and the Department of Biomedical Sciences, Universiti Putra Malaysia, Malaysia and the Discipline of Chemistry, University of Newcastle and the Calvary Mater Hospital, Australia for their facilities. Sunway University Sdn Bhd is thanked for X-ray crystallographic analysis and financial support (Grant. no. STR-RCTR-RCCM-001-2019).

E.N.M.Y. wishes to thank Ministry of Higher Education Malaysia for the award of MyPhD, MyBrain15 and the University of Newcastle for the award of University of Newcastle International Postgraduate Research Scholarship. We would also like to thank Karen A. Crouse, Robert Burns and Adam McCluskey for helpful discussions.

Conflicts of Interest: The authors declare no conflict of interest.

References

[1] G. Domagk, R. Behnisch, F. Mietzsch, H. Schimidt, Naturwissenschaften. 33 (1946) 315.

[2] H. Beraldo, D. Gambino, Mini Rev. Med. Chem. 4 (2004) 31–39.

[3] H.L. Singh, A.K. Varshney, Appl. Organomet. Chem. 15 (2001) 762–768.

[4] E.C. Moore, M.S. Zedeck, K.C. Agrawal, A.C. Sartorelli, Biochemistry. 9 (1970) 4492–4498.

[5] K. Fent, Crit. Rev. Toxicol. 26 (1996) 1–117.

[6] M. Jain, S. Gaur, V.P. Singh, R. V Singh, Appl. Organomet. Chem. 18 (2004) 73–82.

[7] K. Liu, H. Yan, G. Chang, Z. Li, M. Niu, M. Hong, Inorg. Chim. Acta. 464 (2017) 137–146.

[8] M.A. Salam, M.A. Hussein, I. Ramli, S. Islam, J. Organomet. Chem. 813 (2016) 71–77.

[9] R. Singh, N.K. Kaushik, Spectrochim. Acta - Part A Mol. Biomol. Spectrosc. 71 (2008) 669–675.

[10] M. Tariq, S. Ali, N. Muhammad, N.A. Shah, M. Sirajuddin, M.N. Tahir, N. Khalid, M.R. Khan, J. Coord. Chem. 67 (2014) 323–340.

[11] A. Kumar, P. Chaudhary, R. Singh, N.K. Kaushik, Main Group Chem. 15 (2016) 163–178.

[12] A. Bacchi, A. Bonardi, M. Carcelli, P. Mazza, P. Pelagatti, C. Pelizzi, G. Pelizzi, C. Solinas, F. Zani, J. Inorg. Biochem. 69 (1998) 101–112.

[13] Y.F. Win, C.S. Choong, J.C. Dang, M.A. Iqbal, C.K. Quah, A.M.S.A. Majid, S.G. Teoh, J. Coord. Chem. 67 (2014) 3401–3413.

[14] R. Malhotra, A. Ravesh, V. Singh, Phosphorus Sulfur Silicon Relat. Elem. 192 (2017) 73–80.

[15] M. Sirajuddin, S. Ali, V. Mckee, M. Sohail, H. Pasha, Eur. J. Med. Chem. 84 (2014)

343–363.

[16] T. Sedaghat, A. Golalzadeh, H. Motamedi, Phosphorus, Sulfur Silicon Relat. Elem. 188 (2013) 1694–1702.

[17] M. Gielen, Appl. Organomet. Chem. 16 (2002) 481–494.

[18] M. Gielen, M. Biesemans, R. Willem, Appl. Organomet. Chem. 19 (2005) 440–450.

[19] H.L. Singh, J.B. Singh, S. Bhanuka, Res. Chem. Intermed. 42 (2016) 997–1015.

[20] M. Khandani, T. Sedaghat, N. Erfani, M.R. Haghshenas, H.R. Khavasi, J. Mol. Struct. 1037 (2013) 136–143.

[21] J. Wiecek, V. Dokorou, Z. Ciunik, D. Kovala-Demertzi, Polyhedron. 28 (2009) 3298–3304.

[22] M.A. Salam, M.A. Affan, M.A. Arafat, R. Saha, R. Nasrin, Heteroat. Chem. 24 (2013) 43–52.

[23] R.A. Haque, M.A. Salam, M.A. Arafath, J. Coord. Chem. 68 (2015) 2953–2967.

[24] M.A. Salam, A. Arafath, M.A. Hussein, R. Basri, R. Pervin, Phosphorus Sulfur Silicon Relat. Elem. 191 (2016) 1101–1107.

[25] E.N.M. Yusof, M.A.M. Latif, M.I.M. Tahir, J.A. Sakoff, M.I. Simone, A.J. Page, A. Veerakumarasivam, E.R.T. Tiekink, T.B.S.A. Ravoof, Int. J. Mol. Sci. 20 (2019) 854.

[26] E.N.M. Yusof, M.A.M. Latif, M.I.M. Tahir, J.A. Sakoff, A. Veerakumarasivam, A.J. Page, E.R.T. Tiekink, T.B.S.A. Ravoof, J. Mol. Struct. 1205 (2020) 127635.

[27] P. Kalaivani, R. Prabhakaran, E. Ramachandran, F. Dallemer, G. Paramaguru, R. Renganathan, P. Poornima, V. Vijaya Padma, K. Natarajan, Dalton Trans. 41 (2012) 2486–2499.

[28] I. Đilović, M. Rubčić, V. Vrdoljak, S.K. Pavelić, M. Kralj, I. Piantanida, M. Cindrić, Bioorg. Med. Chem. 16 (2008) 5189–5198.

[29] A.T. Swesi, Y. Farina, I. Baba, Sains Malays. 36 (2007) 21–26.

[30] A.T. Swesi, Y. Farina, M. Kassim, S.W. Ng, Acta Crystallogr. Sect. E Struct. Reports Online. E62 (2006) o5457–o5458.

[31] Rigaku Oxford Diffraction. CrysAlis PRO. Agilent Technologies Inc., Santa Clara, CA, USA 2015.

[32] G.M. Sheldrick, Acta Crystallogr. Sect. C Struct. Chem. C71 (2015) 3–8.

[33] G.M. Sheldrick, Acta Crystallogr. Sect. A Found. Crystallogr. A64 (2008) 112–122.

[34] L.J. Farrugia, J. Appl. Crystallogr. 45 (2012) 849–854.

[35] K. Brandenburg, DIAMOND, Crystal Impact GbR, (2006).

[36] A.L. Spek, Acta Crystallogr. Sect. E Crystallogr. Commun. E76 (2020) 1–11.

[37] M.J. Frisch, G.W. Trucks, H.B. Schlegel, G.E. Scuseria, M.A. Robb, J.C. R., G. Scalmani, V. Barone, G.A. Petersson, H. Nakatsuji, X. Li, M. Caricato, A. Marenich, J. Bloino, B.G. Janesko, R. Gomperts, B. Mennucci, H.P. Hratchian, J. V. Ortiz, A.F. Izmaylov, J.L. Sonnenberg, D. Williams-Young, F. Ding, F. Lipparini, F. Egidi, J. Goings, B. Peng, A. Petrone, T. Henderson, D. Ranasinghe, V.G. Zakrzewski, J. Gao, N. Rega, G. Zheng, W. Liang, M. Hada, M. Ehara, K. Toyota, R. Fukuda, J. Hasegawa, M. Ishida, T. Nakajima, Y. Honda, O. Kitao, H. Nakai, T. Vreven, K. Throssell, J.A. Montgomery, Jr., J.E. Peralta, F. Ogliaro, M. Bearpark, J.J. Heyd, E. Brothers, K.N. Kudin, V.N. Staroverov, T. Keith, R. Kobayashi, J. Normand, K. Raghavachari, A. Rendell, J.C. Burant, S.S. Iyengar, J. Tomasi, M. Cossi, J.M. Millam, M. Klene, C. Adamo, R. Cammi, J.W. Ochterski, R.L. Martin, K. Morokuma, O. Farkas, J.B. Foresman, D.J. Fox, Gaussian 09, Revision D.01, Wallingford CT. (2013).

[38] D. Roy, K. Todd, M. John, GaussView, Ver 5.0.9, (2009).

[39] C. Lee, W. Yang, R.G. Parr, Phys. Rev. B. 37 (1988) 785–789.

[40] A.D. Becke, J. Chem. Phys. 98 (1993) 5648–5652.

[41] P.J. Hay, W.R. Wadt, J. Chem. Phys. 82 (1985) 270–283.

[42] P.J. Hay, W.R. Wadt, J. Chem. Phys. 82 (1985) 299–310.

[43] W.R. Wadt, P.J. Hay, J. Chem. Phys. 82 (1985) 284–298.

[44] P.M. Jeffrey, M. Damian, L. Radom, J. Phys. Chem. A. 111 (2007) 11683–11700.

[45] K.-Y. Chen, H.-Y. Tsai, Int. J. Mol. Sci. 15 (2014) 18706–18724.

[46] G. Scalmani, M.J. Frisch, B. Mennucci, J. Tomasi, R. Cammi, V. Barone, J. Chem. Phys. 124 (2006) 94107.

[47] E. Cancès, B. Mennucci, J. Tomasi, J. Chem. Phys. 107 (1997) 3032–3041.

[48] J. Tomasi, M. Persico, Chem. Rev. 94 (1994) 2027–2094.

[49] J. Tomasi, B. Mennucci, R. Cammi, Chem. Rev. 105 (2005) 2999–3093.

[50] L.R. Odell, M.K. Abdel-Hamid, T.A. Hill, N. Chau, K.A. Young, F.M. Deane, J.A. Sakoff, S. Andersson, J.A. Daniel, P.J. Robinson, A. McCluskey, J. Med. Chem. 60 (2017) 349–361.

[51] J. Gilbert, G.N. De Iuliis, M. Tarleton, A. McCluskey, J.A. Sakoff, Mol. Pharmacol. 93 (2018) 168–177.

[52] J.A. Sakoff, S.P. Ackland, Cancer Chemother. Pharmacol. 46 (2000) 477–487.

[53] A.M. Bergman, V.W.T.R. van Haperen, G. Veerman, C.M. Kuiper, G.J. Peters, Clin. Cancer Res. 2 (1996) 521–530.

[54] V. Vrdoljak, M. Cindrić, D. Milić, D. Matković-Čalogović, P. Novak, B. Kamenar, Polyhedron. 24 (2005) 1717–1726.

[55] F.V. Rocha, C.V. Barra, A.E. Mauro, I.Z. Carlos, L. Nauton, M. El Ghozzi, A. Gautier,

L. Morel, A.V.G. Netto, Eur. J. Inorg. Chem. (2013) 4499–4505.

[56] W.J. Geary, Coord. Chem. Rev. 7 (1971) 81–122.

[57] P.M. Krishna, B.S. Shankara, N.S. Reddy, Hindawi. (2013) 1–11.

[58] Y. Matsuda, T. Ebata, N. Mikami, J. Chem. Phys. 110 (1999) 8397.

[59] F. Wang, H. Yin, J. Cui, Y. Zhang, H. Geng, M. Hong, J. Organomet. Chem. 759 (2014) 83–91.

[60] J.M. Galván-Hidalgo, G.M. Chans, T. Ramírez-Apan, A. Nieto-Camacho, S. Hernández-Ortega, E. Gómez, Appl. Organomet. Chem. (2017) 1–12.

[61] Naqeebullah, Y. Farina, K.M. Chan, L.K. Mun, N.F. Rajab, T.C. Ooi, Molecules. 18 (2013) 8696–8711.

[62] H.B. Shawish, M. Paydar, C.Y. Looi, Y.L. Wong, E. Movahed, S.N.A. Halim, W.F. Wong, M.R. Mustafa, M.J. Maah, Transit. Met. Chem. 39 (2014) 81–94.

[63] J. Holeček, M. Nádvorník, K. Handlíř, A. Lyčka, J. Organomet. Chem. 315 (1986) 299–308.

[64] X. Shang, X. Meng, E.C.B.A. Alegria, Q. Li, C. Guedes, M.L. Kuznetsov, A.J.L. Pombeiro, Inorg. Chem. 50 (2011) 8158–8167.

[65] M. Nath, P.K. Saini, A. Kumar, J. Organomet. Chem. 695 (2010) 1353–1362.

[66] M. Hong, G. Chang, R. Li, M. Niu, New J. Chem. 40 (2016) 7889–7900.

[67] S. Yadav, I. Yousuf, M. Usman, M. Ahmad, F. Arjmand, S. Tabassum, RSC Adv. 5 (2015) 50673–50690.

[68] M. Sirajuddin, S. Ali, M.N. Tahir, Inorg. Chim. Acta. 439 (2016) 145–158.

[69] A.W. Addison, T.N. Rao, J. Chem. Soc., Dalton Trans. 7 (1984) 1349–1356.

[70] M. Rubčić, I. Dstrokeilović, M. Cindrić, D. Matković-Čalogović, Acta Crystallogr. Sect. C Cryst. Struct. Commun. 64 (2008) o570–o573.

[71] L.R. Gomes, J.N. Low, N.R.D.L. Correira, T.C.M. Noguiera, A.C. Pinheiro, M.V.N. De Souza, J.L. Wardell, S.M.S.V. Wardell, Zeitschrift Fur Krist. - Cryst. Mater. 234 (2019) 59–71.

[72] R. Lu, W. Wang, X. Lü, S. Zhao, Acta Crystallogr. Sect. E Struct. Reports Online. 67 (2011) o2702.

[73] E.R.T. Tiekink, Coord. Chem. Rev. 345 (2017) 209–228.

[74] D.P. Malenov, G. V. Janjić, V.B. Medaković, M.B. Hall, S.D. Zarić, Coord. Chem. Rev. 345 (2017) 318–341.

[75] N.W. Alcock, Adv. Inorg. Chem. Radiochem. 15 (1972) 1–58.

[76] E.R.T. Tiekink, Appl. Organomet. Chem. 5 (1991) 1–23.

[77] T.S. Basu Baul, A. Paul, L. Pellerito, M. Scopelliti, P. Singh, P. Verma, A. Duthie, D. de Vos, E.R.T. Tiekink, Invest. New Drugs. 29 (2011) 285–299.

[78] F. Arjmand, G.C. Sharma, F. Sayeed, M. Muddassir, S. Tabassum, J. Photochem. Photobiol. B Biol. 105 (2011) 167–174.

[79] B.J. Sishc, C.B. Nelson, M.J. Mckenna, C.L.R. Battaglia, C. Tanzarella, Front. Oncol. 5 (2015) 1–19.

[80] J.H. De Jong, H.M. Rodermond, C.D. Zimberlin, V. Lascano, F.D.S.E. Melo, D.J. Richel, J.P. Medema, L. Vermeulen, Sci. Rep. 2 (2012) 271.

Highlights

- Thiosemicarbazone Schiff bases **1** and **4** are useful lead candidates for future organic drug design development to treat cancers.
- Trigonal bipyramidal diphenyltin(IV) compounds **5, 8, 11** and **14** exhibited excellent cytotoxic activity against the panel of ten cancer cell lines tested, but minimal toxicity against MCF-10A (normal breast).

Graphical Abstract

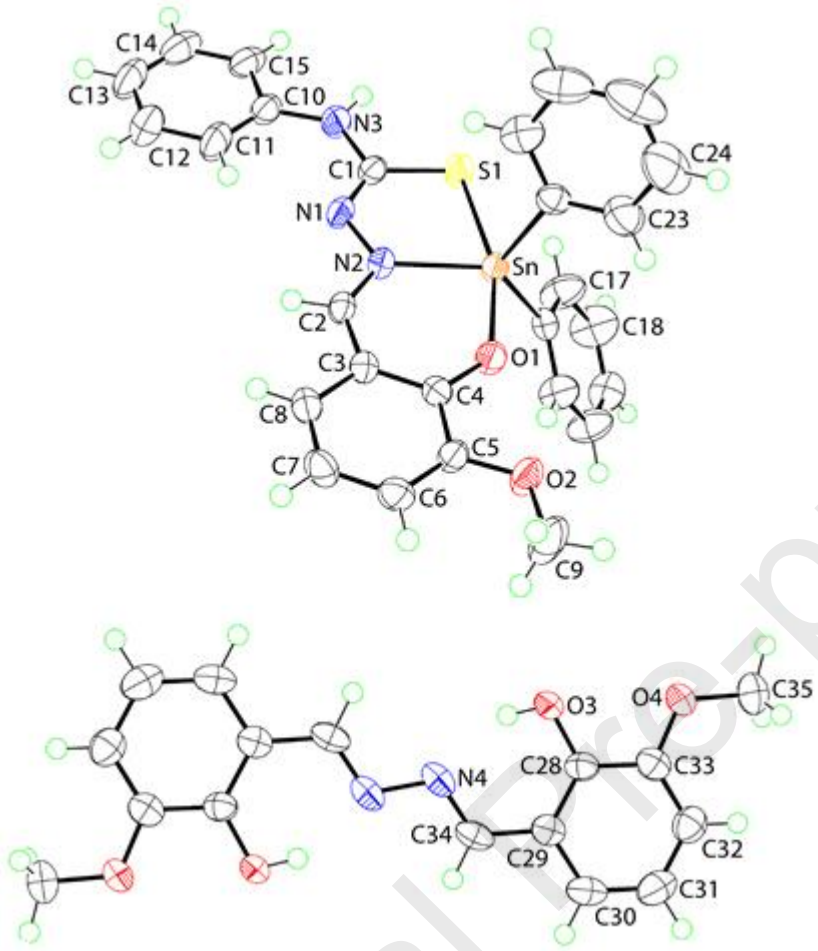

Credit Author Statement

Enis Nadia Md Yusof Formal analysis, Investigation, Data Curation, Writing - Original Draft, Visualization

Alister J. Page Software, Formal analysis, Resources, Data Curation, Writing - Review & Editing,, Visualization, Supervision, Project administration

Jennette A. Sakoff Formal analysis, Resources, Data Curation, Writing - Review & Editing

Michela I. Simone Validation, Formal analysis, Data Curation, Writing - Review & Editing

Abhi Veerakumarasivam Formal analysis, Resources, Data Curation, Writing - Review & Editing, Supervision, Funding acquisition

Edward R. T. Tiekink Software, Formal analysis, Data Curation, Writing - Review & Editing, Visualization

Thahira B. S. A. Ravoof Conceptualization, Methodology, Resources, Writing - Review & Editing, Supervision, Project administration, Funding acquisition